PERGAMON

Journal of the Mechanics and Physics of Solids
49 (2001) 469–511

JOURNAL OF THE
MECHANICS AND
PHYSICS OF SOLIDS

www.elsevier.com/locate/jmps

Feeding and dissipative waves in fracture and phase transition
I. Some 1D structures and a square-cell lattice

L.I. Slepyan*

Department of Solid Mechanics, Materials and Structures, Faculty of Engineering, Tel Aviv University, P.O. Box 39040, Ramat Aviv 69978 Tel Aviv, Israel

Received 3 April 2000; received in revised form 31 July 2000; accepted 13 October 2000

Abstract

In the lattice structure considered here, crack propagation is caused by *feeding* waves, carrying energy to the crack front, and accompanied by *dissipative* waves carrying a part of this energy away from the front (the difference is spent on the bond disintegration). The feeding waves differ by their wavenumber. A zero feeding wavenumber corresponds to a macrolevel-associated solution with the classical homogeneous-material solution as its long-wave approximation. A non-zero wavenumber corresponds to a genuine microlevel solution which has no analogue on the macrolevel. In the latter case, on the crack surfaces and their continuation, the feeding wave is located behind (ahead) the crack front if its group velocity is greater (less) than the phase velocity. Dissipative waves, which appear in both macrolevel-associated and microlevel solutions, are located in accordance with the opposite rule. (Wave dispersion is the underlying phenomenon which allows such a wave configuration to exist.) In contrast to a homogeneous material model, both these solutions permit supersonic crack propagation. Such feeding and dissipative waves and other lattice phenomena are characteristic of dynamic phase transformation as well. In the present paper, mode III crack propagation in a square-cell elastic lattice is studied. Along with the lattice model, some simplified one-dimensional structures are considered allowing one to retrace qualitatively (with no technical difficulties) the main lattice phenomena.

Keywords: A. Dynamics; B. Crack mechanics; Lattice; C. Integral transforms

* Tel.: +972-3640-6224; fax: +972-3640-7617.
E-mail address: leonid@eng.tau.ac.il (L.I. Slepyan).

0022-5096/01/$ - see front matter
PII: S0022-5096(00)00064-8

Nomenclature

a	distance between point particles
c	$=\sqrt{a^2\mu/M}$ speed of a long shear wave
$f^{\mathrm{F}}(k)$	$=\int_{-\infty}^{\infty} f(\eta)\mathrm{e}^{\mathrm{i}k\eta}\,\mathrm{d}\eta$ [also, $f^{\mathrm{F}*}(k)$]
$f^{\mathrm{LF}}(s,k)$	$=\int_{-\infty}^{\infty}\int_{0}^{\infty} f(t,x)\mathrm{e}^{-st+\mathrm{i}kx}\,\mathrm{d}t\,\mathrm{d}x$ or $\sum_{m=-\infty}^{\infty}\int_{0}^{\infty} f(t,x)\mathrm{e}^{-st+\mathrm{i}km}\,\mathrm{d}t$
$f^{\mathrm{LF}*}(s,k)$	$=\int_{-\infty}^{\infty}\int_{0}^{\infty} f(t,\eta)\mathrm{e}^{-st+\mathrm{i}k\eta}\,\mathrm{d}t\,\mathrm{d}\eta$
G	global (macrolevel) energy release rate
G_0	local (microlevel) energy release rate
$H(\eta)$	the unit step function
$h(k)$	$=[2(1-\cos k)+(0+\mathrm{i}kV)^2]^{1/2}$
h_v	non-negative zeros of the function $h(k): h(\pm h_v)=0$
$\Im$	imaginary part of
k	wavenumber and parameter of the Fourier transform
$L(k)$	$=r(k)/h(k)=L_+L_-$
$L_+(L_-)$	has neither singular nor zero points in the upper (lower) half-plane k these subscripts also denote one-side Fourier transform for $\eta\geq 0$ ($\eta\leq 0$)
M	mass of a particle in a lattice or chain
m	number of a particle in a line parallel to the crack in the lattice
n	number of a line of particles; the crack propagates between the lines $n=0,1$
p	internal force in a bond on the crack path
q	external force
R	$=G-G_0$ wave resistance to crack propagation
$\mathscr{R}$	$=\exp\left(\frac{1}{\pi}\int_0^{\infty}\frac{\mathrm{Arg}\,L(\xi)}{\xi}\,\mathrm{d}\xi\right)$
$\Re$	real part of
$r(k)$	$=[4+h^2(k)]^{1/2}$
r_v	non-negative zeros of the function $r(k): r(\pm r_v)=0$
s	parameter of the Laplace transform
t	time
u	displacement of a particle
V	$=v/c$
v	speed of the crack
V_{g}	$=v_{\mathrm{g}}/c$
v_{g}	group velocity of a wave
w	transversal displacement of a one-dimensional structure
x	coordinate (in the case of the lattice, $x=am$ and it is parallel to the crack)
y	$=an$ coordinate normal to the crack
α	creep time
δ	Dirac delta-function
η	$=x-vt$ for continuous x, and $=(x-vt)/a$ for discrete $x=am$
μ	stiffness of a bond and shear modulus
σ	stress
Λ	elongation of a bond
Ω	$=kV$ non-dimensional frequency of a wave

1. Introduction

It is convenient to split the general problem of the crack growth into two. The first is the determination of the crack-behavior-dependent energy flux through the propagating crack tip, while the second concerns the energy required for the crack growth. Generally speaking, the boundary between these *external* (*macrolevel*) and *internal* (*microlevel*) problems is conditional. For example, oscillations in the crack velocity can be referred to the macrolevel, as the phenomenon decreasing the energy flux to the crack, or to the microlevel as the phenomenon which increases the effective surface energy. We hold the latter viewpoint, namely, we consider the first problem in the framework of a homogeneous-material model, as a medium with no wave dispersion, which governs a smoothed crack trajectory and a slowly varying speed.

If the effective surface energy is taken to be known the macrolevel formulation becomes closed. Most theoretical works in fracture are based on this assumption (see Freund, 1990; Broberg, 1999). However, in some cases, especially in crack dynamics, the effective surface energy is hard to be considered as a constant, and the classical energy criterion turns out to be inconsistent with the experiments (see, for example, Ravi-Chandar and Knauss, 1984). Beside, some important phenomena inherent in dynamic fracture cannot be found if the analysis is based on the homogeneous-material model.

An alternative way is the use of a lattice model. A periodic discrete lattice can model a molecular lattice as well as a continous structured material. (From the dynamics point of view, it is important that such a model represents a system with wave dispersion.) In particular, it can serve for the determination of the effective surface energy. For this goal, the steady-state crack propagation studies are sufficient, while the results can be used in the first problem for transient processes.

The lattice studies are known as *molecular dynamics* (see Abraham and Gao, 2000), where numerical technique is used for a nonlinear lattice. Another way is an analytical analysis of linearly elastic and viscoelastic lattices (see Slepyan et al., 1999). It is clear that these two ways can complement each other. In particular, solutions for the super-critical crack speed were found in Abraham and Gao (2000) as well as in Slepyan (1981b). The latter approach is used below.

In the lattice model, similar phenomena in fracture and phase-transition (FPT) are revealed (the phase transition is the subject of Part II of the present work). In the first work in this topic (Slepyan, 1981a), a square-cell lattice consisting of point particles connected by massless elastic bonds was considered and the total radiation by a uniformly propagating crack was analytically determined. A phase-transition wave in a discrete chain consisting of bistable irreversible elements was considered by Slepyan and Troyankina (1984, 1988). A survey of the relevant works in this topic was represented by Slepyan (1998) (also see Slepyan et al., 1999; Slepyan, 2000). In addition to the radiation, the use of the lattice model allows one to reveal the existence of *microlevel solutions* which cannot be found in the homogeneous-medium model. In these works, the following main phenomena were revealed.

Crack-speed-dependent radiation of high-frequency waves excited by the propagating crack front; the radiation intensity does not disappear in the zero crack speed limit, has a global minimum and tends to infinity when the speed approaches a critical

value. It creates wave resistance to crack propagation as a positive difference between the global (macrolevel) and local (microlevel) energy release rate. (The global rate is given by a long-wave asymptotic approximation of the macrolevel-associated lattice solution.) Also, the radiation can lead to damage of the crack surfaces (Marder and Gross, 1995), thus increasing the resistance. The radiation was also analytically determined for phase-transition waves in piecewise linear and nonlinear bistable chains (Slepyan and Troyankina, 1984, 1988).

Supersonic crack propagation is not forbidden in a lattice where the crack can take energy from the initially stressed neighboring layers or from a wave (Slepyan, 1981b).

A structure-associated dynamic amplification factor appears to be a governing phenomenon in FTP (Slepyan, 2000). In a viscoelastic lattice, cracks can grow slowly (Slepyan et al., 1999). This is valid if the relaxation and creep times belong to a static-amplitude-response domain where the dynamic factor does not manifest itself (Slepyan, 2000). Otherwise, in particular, in an elastic lattice, cracks cannot grow slowly [Slepyan (1981a) noted that slow propagation is unstable; Marder and Gross (1995) have shown that it cannot take place].

The instability of a fast straight-line crack is shown (Marder and Gross, 1995).

A size effect in fracture as a strong influence of the cell size is revealed in the viscoelastic lattice model (Slepyan et al., 1999; Slepyan, 2000).

We also refer to three recent manuscripts (Pechenik et al., 2000a, b; Kessler and Levine, 2000) where square-cell and triangular-cell viscoelastic (Kelvin viscosity) lattices are considered for fracture modes I and III.

In the present paper, a complete set of steady-state solutions for mode III crack propagation in a square-cell lattice is represented. The above-mentioned solutions (Slepyan, 1981a, b) obtained for the crack line ($y=0$) are developed for the x, y-plane. A current version of the analytical technique is described in detail (in contrast to these early papers). The crack propagation is considered as a sequence of the bond breaking caused by *feeding* waves, carrying energy to the crack front, and accompanied by *dissipative* waves carrying a part of this energy away from the front (the difference is spent on the bond disintegration). The final expressions for all possible feeding waves are represented. Fast and slow decreasing dissipative waves are shown.

Along with the lattice, we consider some simplified one-dimensional structures allowing one to retrace qualitatively (with no technical difficulties), the main phenomena present in the lattice. In particular, these structures demonstrate the structure- and speed-dependent radiation and different types of feeding and dissipative waves. Also, the wave transformation at the moving phase-separation point and a strong influence of viscosity on the speed of this point can be seen. In connection with the last phenomenon, we note that the 'set of oscillators' (Section 2.2) represents the first explicit solution of the dynamic factor manifestation in the process of such a kind. Indeed, in the paper (Slepyan, 2000), where this insight is introduced, only the separation of domains (on the plane of the creep and relaxation times) is shown, such that slow FPT is possible in one of them and impossible in another.

In a macrolevel-associated solution which contains the well-known homogeneous-material solution as its long-wave asymptote, the feeding wavenumber is equal to zero, while each of the dissipative waves is of a non-zero wavenumber. A microlevel

solution which has no analogue in a homogeneous continuum is characterized by a nonzero feeding wavenumber. In this case, one of the dissipative waves is of the same wavenumber and a zero wavenumber wave carrying energy away from the crack tip can exist. In agreement with its role in the process, the feeding wave considered on the crack surfaces and their continuation is located behind (ahead) the crack front if its group velocity is greater (less) than the phase velocity. The feeding wave destroys the crack-front bonds, one after another, and this gives rise to dissipative waves which are located in accordance with the opposite rule. Note that wave dispersion is the underlying phenomenon which allows such a wave configuration to exist.

The considered lattice is a periodic set of point masses connected by massless bonds which are assumed to be linearly elastic up to the break. Thus they do not have a softening branch in the force–strain relation. In this connection note that the existence of such a branch can lead to a decrease of the energy dissipation. At the same time, the configuration of the feeding and dissipative waves found for the simplified model is still valid for the softening type lattice as well. Indeed, under regular conditions, softening can show itself only in a vicinity of the crack front and hence it can influence the wave amplitude but not the dispersion relations. Thus, the same set of the feeding and dissipative waves corresponds to a given crack speed in both cases.

The technique used in this paper allows one to determine the bond elongation at the moment of its break. However, as shown in Marder and Gross (1995) for a slow crack in an elastic lattice, the maximal strain is achieved earlier and this evidences that the crack cannot propagate slowly (the nature of this phenomenon is discussed in detail in Slepyan, 2000). From this point of view, the corresponding range of the crack speed is forbidden. Nevertheless, we find it reasonable to represent the complete solution including that for the 'forbidden region'. In fact, the solution corresponds to the cutting of the bonds with a given speed, and how it relates to the crack propagation under remote forces is the matter of the type of the fracture criterion. At the same time, in some cases, we determine the conditions (including the crack speed) which justify the solution under the limiting-strain criterion.

2. Three simple models

2.1. Thread-beam problem

The thread-beam model can serve as the simplest example to illustrate the importance of a structure which needs to be taken into account in the determination of energy fluxes. Furthermore, this model incorporates the macrolevel-associated and microlevel-type solutions. Note that we call a model with (without) wave dispersion as the *macrolevel* (*microlevel*). This simple example, but without the microlevel solution, was first introduced in Slepyan (1984). A related problem of splitting of a beam with a wedge was considered by Freund (1990).

Consider an inclined thread falling on a rigid foundation (Fig. 1). In this process, a point uniformly moving with speed $v > 0$ separates the falling thread at the right and

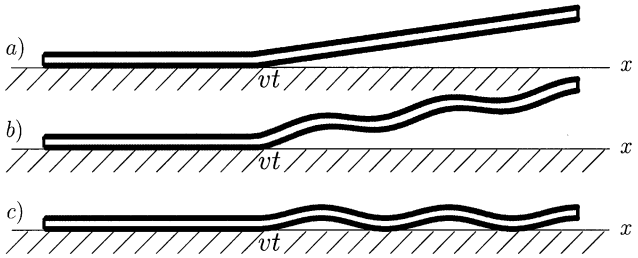

Fig. 1. The thread-beam problem: (a) the macrolevel solution ($EI=0$), (b) the macrolevel-associated solution ($EI>0$), (c) the microlevel solution ($EI>0$).

the contact zone at the left where the thread is assumed to be at rest. The angle, ψ, between the falling thread and the foundation is assumed to be small enough to allow the difference in length between an element of the thread and its projection onto the foundation to be neglected. Conditionally, this process could be referred to as 'crack closing'.

Taking into account possible bending stiffness of the thread, its dynamic equation can be represented as for a beam

$$EI\frac{\partial^4 w}{\partial x^4}+\rho A\frac{\partial^2 w}{\partial t^2}=q, \tag{1}$$

where w is the lateral displacement directed to the foundation, EI is the bending stiffness (E is the elastic modulus); x, t, ρ, A and q are the coordinate along the thread (or the foundation), time, density, cross-sectional area and external loading, respectively. The loading is constituted by the contact thread-foundation force ($q<0$ in compression).

The thread can be considered as a non-structured one-dimensional continuum if the bending stiffness is negligible. This can be referred to the macrolevel representation of the body where there is no wave dispersion. In contrast, the formulation with a positive bending stiffness is referred to the microlevel. In this latter case, there exists the wave dispersion associated with the bending stiffness.

First, consider the problem under the condition $EI=0$ (Fig. 1a). In this case, there exists an energy release rate equal to the kinetic energy of the thread per unit length. This energy is released through the moving contact point, $x=vt$. The solution to this problem can be expressed as

$$w=w_0=-\psi\,\eta H(\eta)\quad(\eta=x-vt), \tag{2}$$

where H is the unit step function. The particle velocity $\dot{w}_0$, the moving load q and the energy release G are

$$\dot{w}_0=\psi\,vH(\eta),\quad q=-\rho A\psi\,v^2\delta(\eta),\quad G=G_0=\tfrac{1}{2}\rho A(\psi\,v)^2. \tag{3}$$

Now consider the 'structured' thread, that is, the thread with a positive bending stiffness. A general solution to this problem consists of two terms:

$$
\begin{aligned}
&w = w_1 + w_2,\\
&w_1 = -\psi\left[\eta - \frac{1}{k}\sin(k\,x - \omega t)\right]H(\eta),\\
&w_2 = C[1 - \cos(k\,x - \omega t)]H(\eta),\\
&k = v\sqrt{\frac{\rho A}{EI}}, \quad \omega = \sqrt{\frac{EI}{\rho A}}k^2 = v^2\sqrt{\frac{\rho A}{EI}} \ \ (k\,x - \omega t \equiv k\eta),
\end{aligned}
\tag{4}
$$

where C is an arbitrary constant. The first term results in the particle velocity, contact force and energy release rate as follows:

$$
\dot{w}_1 = \psi\, v[1 - \cos(k\eta)]H(\eta), \quad q = q_1 = -\rho A\psi\, v^2\delta(\eta), \quad G = G_1 = 0. \tag{5}
$$

This is a macrolevel-associated solution: $w_1 \to w_0$ ($EI \to 0$). This solution is represented in Fig. 1b.

The second term (see Fig. 1c) gives

$$
\dot{w}_2 = Ck\sin(k\eta)H(\eta), \quad q = q_2 = C\rho A v^2\delta'(\eta), \quad G = G_2 = -C^2\frac{v^4}{2}\frac{(\rho A)^2}{EI}. \tag{6}
$$

These results were obtained as follows: the contact compressive force was determined by substitution of solution (4) into dynamic Eq. (1), while the energy release is defined as

$$
\begin{aligned}
&G_1 = \psi^2\rho A\frac{v^2}{2} - \frac{N}{v}, \quad G_2 = -\frac{N}{v}, \quad N = (v_g - v)W,\\
&W = \frac{1}{2}\left[EI\left(\frac{\mathrm{d}^2 w}{\mathrm{d}x^2}\right)^2 + \rho A\dot{w}^2\right], \quad v_g = \frac{\mathrm{d}\omega}{\mathrm{d}k} = 2v,
\end{aligned}
\tag{7}
$$

where N is the energy flux from the moving point $x = vt$, W is energy per unit length and v_g is the group velocity of the bending wave (v is its phase velocity).

Thus, the first term represents the process where the bending wave carries away all the kinetic energy of the thread released during the collision. In this case, there is no energy release but only a transformation: the kinetic energy of the uniformly falling thread goes into energy of the bending wave. If the bending stiffness vanishes, $EI \to 0$, the amplitude of the wave tends to zero and the wave cannot be seen on the macrolevel. However, the energy flux through the moving contact point is still zero independently of the stiffness (if $EI > 0$). It can be concluded that the macrolevel considerations are not sufficient for the determination of the energy fluxes. If one excludes the existence of the microlevel altogether, the kinetic energy flows through the contact point; but if one assumes the existence of the microlevel where $EI > 0$, the path of this energy is dramatically changed: it radiates with the bending wave which can be seen on the microlevel only.

Thus, in the case $EI = 0$, the solution is not uniquely defined since there is energy dissipation at the moving contact point if EI is set to zero a priori, and there is no

dissipation if this equality is considered as a limit. Of course, the radiation can be considered as dissipation also, but only in the case when there is no interest in the details of the energy absorption. Suppose, one needs to obtain a composite with a layer cemented to the plate by such a process. Here, it is important how much energy goes to the contact line and remains there; it is thus seen that it is not too easy to answer this question.

The second term, w_2, defines an arbitrary energy flux (6) along the beam (with $EA > 0$) induced by the work of the generalized force q_2. This hypothetical solution is completely independent of the macrolevel formulation. In contrast to the first term (5) which incorporates the macro- and microlevel processes, it represents a genuine microlevel solution.

One now can reverse the process, that is, consider the negative speed, $v < 0$. In this case, the directions of the energy fluxes become opposite to the above-determined. Now the former macrolevel solution (2) corresponds to the energy flux from the contact point where, due to the work of the force q the thread gains the kinetic energy. The former macrolevel-associated solution, w_1 (4), now represents a process where the bending wave propagating to the left transfers into the uniform motion. Finally, the microlevel solution, w_2 (4), now represents the 'crack propagation' where the energy required for the crack to grow, that is, the fracture energy, goes to the 'crack tip' (to the contact point) by means of the bending wave (this wave is called the feeding wave). In this latter case, the generalized force q_2 (6) serves for the energy consumption.

2.2. Fast and slow phase-transition waves

The dynamic amplification factor plays a governing role in crack and phase-transition wave propagation. This insight was introduced in Slepyan (1999) where conditions allowing a crack or a phase-transition wave to propagate slowly were examined based on discrete lattice and chain structures with the standard-material viscoelastic bonds. The below-considered model, allowing an explicit solution, can serve as a simplest example of such a process.

Consider a periodic set of oscillators each of mass M loaded by a constant force P and let a be the distance between neighboring oscillators (Fig. 2). Each spring is assumed to be viscoelastic with stiffness μ and creep time $\alpha \geq 0$ (the relaxation time is assumed here to be zero). Thus, the dynamic equation of the oscillator is

$$M\frac{\mathrm{d}^2u}{\mathrm{d}t^2} + \mu\alpha\frac{\mathrm{d}u}{\mathrm{d}t} + \mu u = P, \tag{8}$$

where t is time.

In addition to the spring, each mass is assumed to have an intermediate removable support which prevents its displacement. This represents the initial state of the oscillator (referred to 'phase I') with zero displacement and velocity.

Assume the intermediate support to be removed from an oscillator (oscillator A; see Fig. 2) at the moment when the displacement of a neighboring oscillator (oscillator B) reaches a critical value, u_*. After this 'activation' oscillator A moves to 'phase II' where $u = P/\mu$. Under these conditions, a phase-transition wave can propagate along

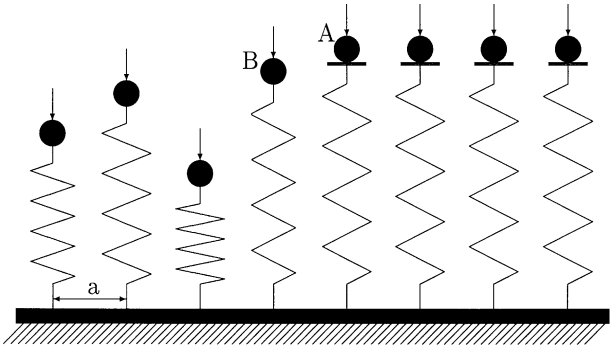

Fig. 2. Periodic set of oscillators.

this chain of oscillators if the force, P, is sufficiently large and the intermediate support of an oscillator is removed by a disturbance. We note that there is no energy flux in this wave because the oscillators interact with each other only by an activation signal carrying no energy.

This simplest structure is of course rather artificial; however, it represents a good model which allows one to retrace qualitatively (with no technical difficulties) the influence of the dynamic factor on the speed of a crack or a phase-transition wave.

Non-dimensional time $t' = t\omega$ ($\omega = \sqrt{\mu/M}$), creep time $\alpha' = \alpha\omega$, displacement $u' = u/u_*$, force $P' = P/P_*$ ($P_* = \mu u_*$) and wave speed $v' = v/(a\omega)$ are used below, but the primes are dropped. In addition, we denote $\phi = \sqrt{1 - \alpha^2/4}$. The following expression for the displacement of the oscillator is valid:

$$u = P\left[1 - \mathrm{e}^{-\alpha t/2}\left(\cos\phi t + \frac{\alpha}{2}\frac{\sin\phi t}{\phi}\right)\right]. \tag{9}$$

If we consider now how the wave speed depends on P and α, an analysis leads to the following conclusions.

An overshoot exists if $\alpha < 2$ [it is the dynamic overshoot response (DOR) domain], and in this case, for any value of α ($0 \le \alpha < 2$) there exists a lower bound $v_{\min} > 0$ of the wave speed v. In contrast, in the case of the static-amplitude-response (SAR) domain ($\alpha \ge 2$), no lower bound exists and the wave can propagate slowly: the wave speed approaches zero as the force, $P > 1$, approaches the critical value $P_c = 1$.

Further, if the creep time belongs to the DOR domain, the wave can propagate even in the case where the force is sub-critical, i.e. $P < 1$. Indeed, consider the elastic case, $\alpha = 0$; here, if the intermediate support is removed at $t = 0$,

$$u = P(1 - \cos t), \tag{10}$$

and it is clear that the wave can propagate if $P \ge 1/2$. The non-dimensional speed is defined as $v = 1/t_0$, where t_0 is the required non-dimensional time for the displacement of the oscillator to reach the critical value. For instance, if $P = 1/2$, then $t_0 = \pi$ and hence $v = 1/\pi$. This is the minimal speed for the elastic case since t_0 decreases as P

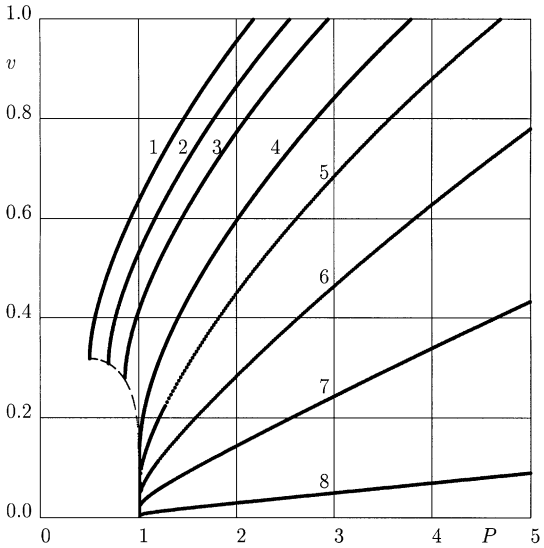

Fig. 3. Force-speed dependence: The DOR domain: 1. $\alpha=0$; 2. $\alpha=0.5$; 3. $\alpha=1$. The SAR domain: 4. $\alpha=2$; 5. $\alpha=3$; 6. $\alpha=5$; 7. $\alpha=10$; 8. $\alpha=50$. The dotted curve: $---$ $v_{\min}$ $(P_{\min})$.

increases. If $0 \leq \alpha \leq 2$ the following dependences for minimal values of P and v are valid:

$$P_{\min}(\alpha)=\left[1+\exp\left(-\frac{\pi\alpha}{2\phi}\right)\right]^{-1}, \quad v_{\min}(\alpha)=\frac{\phi}{\pi},$$

$$P_{\min}=\left[1+\exp\left(-\frac{\sqrt{1-\pi^2 v_{\min}^2}}{v_{\min}}\right)\right]^{-1}. \tag{11}$$

The lower wave speed bound decreases with an increase of α and becomes zero in the SAR domain (including its boundary) where $\alpha \geq 2$. In the latter case, the wave cannot propagate under a sub-critical force because there is no overshoot in the SAR domain. The response of the oscillator, $u(t)$, approaches maximum at infinity and, in contrast to the DOR domain, any sub-critical force leads to a sub-critical displacement.

Plots of the force-speed dependence for several values of α are represented in Fig. 3 (the minimal wave speed, $v_{\min}(P_{\min}), 1/2 < P < 1$, is shown by a dashed curve).

2.3. Energy absorber propagating together with a wave

Consider a string on an elastic foundation under a moving load. This simple model allows one to see how the energy of a wave can be absorbed in a steady-state regime. As shown below the same phenomenon exists in crack propagation in a lattice where the crack can absorb energy from a sinusoidal wave. Also, this concerns a phase-transition process.

Examine the equation

$$Tw'' - \rho A\ddot{w} - \kappa w = -q(x - vt), \tag{12}$$

where T is the tensile force and κ is the stiffness of the foundation. In terms of non-dimensional variables

$$x = \sqrt{\frac{T}{\kappa}}x', \quad w = \sqrt{\frac{T}{\kappa}}w', \quad t = \sqrt{\frac{\rho A}{\kappa}}t', \quad q = \sqrt{T\kappa}q', \quad v = c_0 V, \quad c_0 = \sqrt{\frac{T}{\rho A}}, \tag{13}$$

where c_0 is the sound speed (below the superscript is dropped), the equation becomes

$$w'' - \ddot{w} - w = -q(x - Vt). \tag{14}$$

For a steady-state solution, $w = w(\eta)$, $\eta = x - Vt$, considered as a limit of the corresponding transient solution with zero initial conditions (see Appendix A), the Fourier transform leads to

$$w^{\mathrm{F}} = \frac{q^{\mathrm{F}}}{k^2 + (0 + \mathrm{i}kV)^2 + 1}. \tag{15}$$

Note that there are no propagating waves with non-dimensional phase velocity $V < 1$ and the steady-state solution does not exist for $V = 1$, which is a resonant speed. Letting $V > 1$, $q = q_1\delta(\eta)$ ($q^{\mathrm{F}} = q_1$), one gets:

$$w(\eta) = w_1 = -q_1 k_0 \sin k_0\eta H(-\eta), \quad k_0 = \frac{1}{\sqrt{V^2 - 1}}. \tag{16}$$

Thus, the wave excited by the supersonic moving load is located behind the load. This is a consequence of the fact that the phase velocity of the wave, v, exceeds the group velocity, v_{g}: $V_{\mathrm{g}} = v_{\mathrm{g}}/c = k/\sqrt{1 + k^2} = 1/V$ (see Appendix B).

Note that the work of the load per unit time is positive since the wave carries energy away from the load. This wave can be called the *dissipative* one. In order to calculate the power as the product of the force and particle velocity one can distribute the force in a small segment to obtain a continuous velocity. As a result the non-dimensional power of the force turns out to be

$$N = \frac{Vq_1^2}{2(V^2 - 1)}. \tag{17}$$

We now introduce a free wave

$$w(\eta) = w_0 = q_0 k_0 \sin k_0\eta \quad (\infty < \eta < \infty) \tag{18}$$

as an initial condition. The superposition gives us two waves

$$w_0(\eta) + w_1(\eta) = (q_0 - q_1)k_0 \sin k_0\eta H(-\eta) + q_0 k_0 \sin k_0\eta H(\eta), \tag{19}$$

one of which is located behind the moving force and another ahead the force. Note that work of the force on the latter wave is negative since its group velocity relative

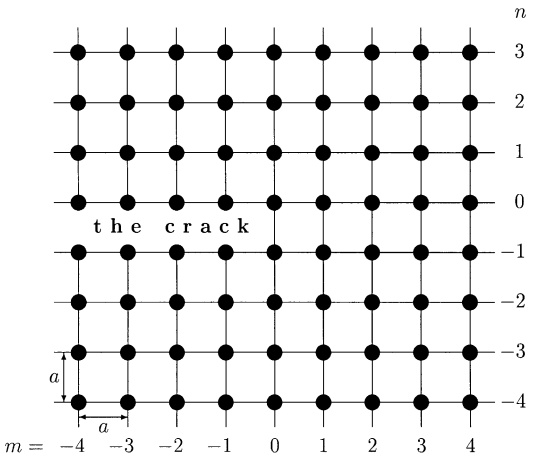

Fig. 4. Square-cell lattice.

to the force velocity, v, is directed towards the force. Thus, the power of the force is now

$$N = \frac{V[(q_0 - q_1)^2 - q_0^2]}{2(V^2 - 1)}. \tag{20}$$

As the amplitude of the initial wave, q_0, increases the power of the force, N, decreases becoming zero when $q_0 = q_1/2$ and then negative when $q_0 > q_1/2$. In particular, if $q_0 = q_1$, only the wave ahead the force remains and its energy flows to the force which plays the role of an energy absorber. Such a wave can be called the *feeding* wave.

Note that $v_g = v/2$ for a wave on the deep-sea surface and it can represent another example of the feeding wave of such a kind.

3. Dynamic crack growth in a square-cell elastic lattice

Consider an infinite lattice consisting of point particles of mass M. Each particle is connected with four neighbors by the same linearly elastic bonds each of length a (Fig. 4). For this lattice mode III crack propagation is studied. A semi-infinite crack is assumed to propagate to the right with constant speed v; that is, the time-interval between the breaking of neighboring bonds on the crack path, a/v, is constant. In this 'steady-state' process, one or several feeding waves can deliver energy to the crack front. A part of the energy is spent on the bond disintegration on the crack path and the rest is radiated by dissipative waves away from the crack front. The number of these waves and their location depend on the crack speed. In outline, the plan of the solution is as follows.

First, the Fourier transformation of the steady-state dynamic equations for an unbounded intact lattice is performed and a general solution is derived. Then a dynamic

equation for a particle on the line $n = 0$ is considered. This equation differs from that for $n > 0$ (or $n < -1$) by the absence of the internal forces acting from below on the particles $n = 0$ on the crack surface and by the presence of external forces which are introduced for convenience in an initial stage of the considerations. As a result, we derive the Wiener–Hopf-type equation as an inhomogeneous relation between the Fourier transforms for the internal forces ahead the crack and the crack opening displacement.

The next step is the determination of the location of singular points of this equation and the factorization of its coefficient as prescribed by the Wiener–Hopf technique. Further, the external forces are eliminated by means of a procedure which leads to an equation with a non-zero right-hand side which reflects the existence of the feeding waves. A general solution of this equation contains a crack-speed-dependent number of singular points the contributions of which define all the feeding and dissipative waves. First, the feeding waves and asymptotes of the dissipative waves are determined for the crack surface and its continuation, $n = 0$, and then, the description of the waves for $n \geq 0$ and $n \leq -1$ is given.

3.1. Derivation of the governing equation

The dynamic equation of the lattice is

$$M\frac{\mathrm{d}^2 u_{m,n}}{\mathrm{d}t^2} = \mu(u_{m+1,n} + u_{m-1,n} + u_{m,n+1} + u_{m,n-1} - 4u_{m,n}), \tag{21}$$

where $u_{m,n}$ are displacements, m and n are horizontal and vertical numbers of a particle, respectively ($m \equiv x/a$, $n \equiv y/a$), and μ is the bond stiffness per unit length in the out-of-plane direction. This equation is valid out of the crack, that is, for $n > 0$ and $n < -1$.

Via a long-wave approximation, the lattice corresponds to a plane homogeneous body of density M/a^2 and shear modulus μ. Accordingly, the shear wave velocity is given by $c = \sqrt{a^2\mu/M}$.

In the following, for a discrete system, we denote

$$\eta = (x - vt)/a = m - vt/a, \tag{22}$$

where η is treated as a continuous variable for each m. Assuming

$$u_n = u_n(\eta), \tag{23}$$

one can rewrite Eq. (21) in the form

$$V^2\frac{\mathrm{d}^2 u_n(\eta)}{\mathrm{d}\eta^2} = [u_n(\eta + 1) + u_n(\eta - 1) + u_{n+1}(\eta) + u_{n-1}(\eta) - 4u_n(\eta)], \quad V = \frac{v}{c}, \tag{24}$$

while in terms of the two-sided Fourier transform

$$(h^2 + 2)u_n^{\mathrm{F}} - (u_{n+1}^{\mathrm{F}} + u_{n-1}^{\mathrm{F}}) = 0, \tag{25}$$

where

$$h^2 = 2(1 - \cos k) + (s + \mathrm{i}kV)^2, \quad r^2 = h^2 + 4 \ \ (s \to +0). \tag{26}$$

In connection with the last limit, see Appendix A (to denote the Fourier transform with respect to η we use here superscript F but not F_* as in Appendix A). The limit is denoted as

$$\lim_{s\to+0}(s+\mathrm{i}kV)=0+\mathrm{i}kV. \tag{27}$$

In the following, we denote the Fourier transforms which have no singular points in the lower (upper) half-plane k by subscript '$-$' ('$+$'). [The corresponding originals of such transforms have support $\eta\le 0$ ($\eta\ge 0$)].

Eq. (25) is satisfied by the expression

$$u_n^{\mathrm{F}}=u^{\mathrm{F}}\lambda_{1,2}^n,\quad u^{\mathrm{F}}=u_0^{\mathrm{F}} \tag{28}$$

with

$$\lambda_1\equiv\lambda=\frac{r-h}{r+h},\quad \lambda_2=\frac{1}{\lambda}. \tag{29}$$

For the problem of a crack in an unbounded lattice, it is assumed that $u_n^{\mathrm{F}}\to 0$ when $n\to\pm\infty$ and hence

$$u_n^{\mathrm{F}}=u^{\mathrm{F}}\lambda^n\ \ (n\ge 0),\quad u_n^{\mathrm{F}}=-u^{\mathrm{F}}\lambda^{-(n+1)}\ \ (n\le -1). \tag{30}$$

Note that $|\lambda|<1$ if s in (26) is positive. Indeed, if $s>0$

$$-\pi<\operatorname{Arg}h^2<\pi,\quad \Re h>0,\quad \Re r>0,\quad \operatorname{sgn}\Im h=\operatorname{sgn}\Im r \tag{31}$$

and it follows that

$$|r-h|<|r+h|. \tag{32}$$

Consider now the line $n=0$. The force acting from below on the particles lying on this line is a sum of a force, $p(\eta)$, as the internal force in the bonds connected particles $n=0$ and $n=-1$ in front of the crack, and an external force, $q(\eta)$. Eq. (21) takes the form

$$M\frac{\mathrm{d}^2u_{m,0}}{\mathrm{d}t^2}+p(\eta)+q(\eta)=\mu(u_{m+1,0}+u_{m-1,0}+u_{m,1}-3u_{m,0}). \tag{33}$$

From this, it follows that

$$p^{\mathrm{F}}=p_+=-\mu[(h^2+1)u^{\mathrm{F}}-u_1^{\mathrm{F}}]-q^{\mathrm{F}} \tag{34}$$

or, using (26)–(30),

$$p_+=-\frac{\mu h(r+h)}{2}u^{\mathrm{F}}-q^{\mathrm{F}}=-\frac{\mu h(r+h)}{2}(u_++u_-)-q^{\mathrm{F}} \tag{35}$$

with $q^{\mathrm{F}}=q_++q_-$. Note that external forces which can act on the particles $n=0$ and $n=-1$ in front of the crack (with q_+ as the Fourier transform) must also be taken into account. This term, q_+, is not present in the case of a homogeneous-material model.

Substituting $u_+=p_+/(2\mu)$ into (35) we obtain the Wiener–Hopf-type equation as

$$\frac{L}{2}p_++\mu u_-=-\frac{L-1}{2}(q_++q_-) \tag{36}$$

with

$$L=\frac{r}{h}. \tag{37}$$

3.2. Zero points of the functions $h(k)$ and $r(k)$

Both the feeding and dissipative waves are associated with zero points of the functions $h(k)$ and $r(k)$ and the determination of these points is a necessary stage in the study of the problem. For $k \to 0$, the function $h^2(k)$ has the following asymptotes:

$$h^2 \sim (1-V^2)(0+\mathrm{i}k)(0-\mathrm{i}k) \quad (0 \le V < 1)$$
$$h^2 \sim (V^2-1)(0+\mathrm{i}k)^2 \quad (V > 1), \tag{38}$$

while for the critical speed $V = 1$ (see Appendix B)

$$h^2 \sim \tfrac{1}{12}(k-k_1)(k-k_2)(k-k_3)(k-k_4) \quad (k \to 0),$$
$$k_m \sim (24s)^{1/3}\exp[\tfrac{1}{3}\mathrm{i}\pi(\tfrac{1}{2}+2(m-1))], \quad m = 1,2,3; \quad k_4 \sim \frac{\mathrm{i}s}{2}\left(\frac{s}{k} \to +0\right). \tag{39}$$

In addition, if $V < 1$ this function has one, three or more pairs of simple zeros at $k \neq 0$: $k = \pm h_1, \pm h_2, \ldots, \pm h_{2l+1}$, where number l increases as V decreases. In particular,

$$l = 0 \quad \text{for } V > V_0 \approx 0.2172. \tag{40}$$

There are no such points for $V \ge 1$. The zeros h_v $(v = 1,2,\ldots)$ form an increasing sequence $h_1 < h_2 < \cdots < h_{2l+1}$. Under certain values of the speed, two neighboring zero points can unite; in the following however, simple zeros are assumed unless noted otherwise. The function h has the following representation in a vicinity of a zero point:

$$h \sim \text{const}\sqrt{0+\mathrm{i}(k-h_{2v-1})} \quad (k \to h_{2v-1}),$$
$$h \sim \text{const}\sqrt{0-\mathrm{i}(k-h_{2v})} \quad (k \to h_{2v}). \tag{41}$$

These representations are in agreement with the corresponding relations between the group and phase velocities of the waves associated with the zero points as their wavenumbers (see Appendix B), namely

$$v_{\mathrm{g}} < v \ \ (k = h_{2v-1}), \quad v_{\mathrm{g}} > v \ \ (k = h_{2v}), \tag{42}$$

where

$$V_{\mathrm{g}} = \frac{v_{\mathrm{g}}}{c} = \frac{\mathrm{d}\Omega}{\mathrm{d}k}, \quad V = \frac{v}{c} = \frac{\Omega}{k}, \quad \Omega^2 = V^2k^2 = 2(1-\cos k). \tag{43}$$

The validity of relations (42) can be easily seen in Fig. 5 where the dispersion curves

$$\Omega(k) = \Omega_h = 2|\sin k/2| \ \ (h = 0), \quad \Omega(k) = \Omega_r = 2\sqrt{1+\sin^2 k/2} \ \ (r = 0) \tag{44}$$

are shown.

The function $\mathrm{Arg}\,h(k)$ is a piecewise constant. In accordance with the representations in (41), when the increasing variable k passes a zero point of h, $\mathrm{Arg}\,h(k)$ exhibits an increase as

$$\Delta\mathrm{Arg}\,h = \frac{\pi}{2} \ \ (k = h_{2v-1}), \quad \Delta\mathrm{Arg}\,h = -\frac{\pi}{2} \ \ (k = h_{2v}). \tag{45}$$

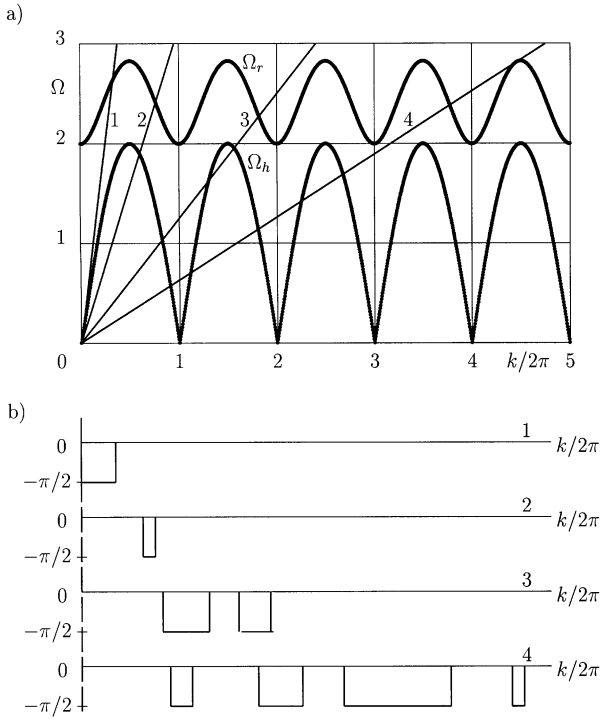

Fig. 5. Dispersion relations (a) and $\operatorname{Arg} L(k)$ (b) 1. $v = 1.5$; 2. $v = 0.5$; 3. $v = 0.2$; 4. $v = 0.1$.

We can assume $\operatorname{Arg} h(0) = 0$. Then for $V < 1$

$$\operatorname{Arg} h = 0 \ [h_{2v-2} < k < h_{2v-1}, (h_0 = 0)], \quad \operatorname{Arg} h = \frac{\pi}{2} \ (h_{2v-1} < k < h_{2v})$$
$$\operatorname{Arg} h = \frac{\pi}{2} \ (k > h_{2l+1}), \quad \operatorname{Arg} h(-k) = -\operatorname{Arg} h(k), \tag{46}$$

while for $V \geq 1$

$$\operatorname{Arg} h = \frac{\pi}{2} \ (k > 0), \quad \operatorname{Arg} h = -\frac{\pi}{2} \ (k < 0). \tag{47}$$

The function $r(k)$ is positive at $k = 0$ $[r(0) = 2]$ and has one, three or more couples of zero points at $k \neq 0$: $k = \pm r_1, \pm r_2, \ldots, \pm r_{2d+1}$ $(d = 0, 1, \ldots; h_{2l+1} < r_1)$. In particular, $d = 0$ for

$$V > V_1 \approx 0.3028. \tag{48}$$

Note that $r_1 > 0$ for any $V < \infty$ in contrast to h_1 which becomes zero when V approaches unity. In other respects, similar statements concerning the zeros of $r(k)$ and $\operatorname{Arg} r$ are valid as for the zeros of function $h(k)$, $k \neq 0$, and $\operatorname{Arg} h$ (46).

3.3. Factorization

One now can see that $\operatorname{Arg} L(k)=0$ for $k^2<h_1^2$ and $k^2>r_{2d+1}^2$, and it is zero or negative in the segment $h_1^2<k^2<r_{2d+1}^2$ (see Fig. 5). Further

$$\Re L(-k)=\Re L(k),\quad \Im L(-k)=-\Im L(k) \tag{49}$$

and

$$\begin{aligned}&\operatorname{Ind} L(k)=\frac{1}{2\pi}[\operatorname{Arg} L(+\infty)-\operatorname{Arg} L(-\infty)]=0,\\ &L(\pm\infty)=1,\quad |\ln L(-k)|=|\ln L(k)|,\quad \operatorname{Arg} L(-k)=-\operatorname{Arg} L(k).\end{aligned} \tag{50}$$

This allows the following representation valid for $V<1$ ($h_1>0$):

$$L(k)=L_+(k)L_-(k) \tag{51}$$

with

$$L_\pm(k)=\exp\left(\pm\frac{1}{2\pi i}\int_{-\infty}^{\infty}\frac{\ln L(\xi)}{\xi-k}\,\mathrm{d}\xi\right), \tag{52}$$

where $\Im k>0$ for the functions marked by subscript '+' and $\Im k<0$ for the functions marked by subscript '−'. In this factorization, L_+ has neither singular nor zero points in the upper half-plane k, while L_- has no such points in the lower half-plane (the half-planes include the real axis if $\Re s>0$). This means that $1/L_+$ and $1/L_-$ are regular in the corresponding half-planes as well as L_+ and L_-.

As follows from their definition (52), equalities (49) are valid for functions $L_\pm(k)$ as well as for $L(k)$. The function $L_+(k)[L_-(k)]$ incorporates the zeros of $h(k)$ and $r(k)$ with $V_g>V$ [$V_g<V$] as its singular points, such that

$$\begin{aligned}&L_+(r_{2v})=0,\quad L_+(h_{2v})=\infty,\\ &L_-(r_{2v-1})=0,\quad L_-(h_{2v-1})=\infty.\end{aligned} \tag{53}$$

The functions L and $L_\pm(k)$ have the following asymptotes:

$$\begin{aligned}&L(k)\sim\frac{2}{\sqrt{1-V^2}\sqrt{(0+\mathrm{i}k)(0-\mathrm{i}k)}}\ (k\to 0),\quad L_\pm(k)\to 1\ (k\to\pm\mathrm{i}\infty),\\ &L_\pm(k)=\sqrt{2}(1-V^2)^{-1/4}(0\mp\mathrm{i}k)^{-1/2}\mathscr{R}^{\pm1}\ (k\to 0)\end{aligned} \tag{54}$$

with

$$\mathscr{R}=\exp\left(\frac{1}{\pi}\int_0^{\infty}\frac{\operatorname{Arg} L(\xi)}{\xi}\,\mathrm{d}\xi\right). \tag{55}$$

Based on (46) and the corresponding relations for $r(k)$ which, together, describe piecewise constant $\operatorname{Arg} L(k)$, we can also represent $\mathscr{R}$ as

$$\mathscr{R}=\left(\prod_{v=1}^{d}r_{2v}\prod_{v=1}^{l+1}h_{2v-1}\right)^{1/2}\left(\prod_{v=1}^{d+1}r_{2v-1}\prod_{v=1}^{l}h_{2v}\right)^{-1/2}\left(\prod_{v=1}^{0}=1\right). \tag{56}$$

In the following, another form of representation (51) will also be useful. Represent

$$L(k)=\frac{R_+(k)R_-(k)}{H_+(k)H_-(k)}S(k), \tag{57}$$

where for $V<1$

$$R_+^2(k)=\prod_{v=1}^{d}\left[1+\left(\frac{r_{2v}}{0-\mathrm{i}k}\right)^2\right],\quad R_-^2(k)=\prod_{v=1}^{d+1}\left[1+\left(\frac{r_{2v-1}}{0+\mathrm{i}k}\right)^2\right],$$
$$H_+^2(k)=\prod_{v=1}^{l}\left[1+\left(\frac{h_{2v}}{0-\mathrm{i}k}\right)^2\right],\quad H_-^2(k)=\prod_{v=1}^{l+1}\left[1+\left(\frac{h_{2v-1}}{0+\mathrm{i}k}\right)^2\right] \tag{58}$$

and for $V\geq 1$

$$R_+=1,\quad R_-^2=\left[1+\left(\frac{r_1}{0+\mathrm{i}k}\right)^2\right],\quad H_+=1,\quad H_-=1. \tag{59}$$

Under this definition of the function $S(k)$, $\operatorname{Arg}S(k)=0$ $(-\infty<k<\infty)$, $S(\pm\infty)=1$ and $\ln S(k)$ is a real locally integrable function. This allows one to factorize this function using the Cauchy type integral (52) with the result

$$S(k)=S_+(k)S_-(k),\quad S_+(k)=\overline{S_-(\bar{k})} \tag{60}$$

and hence on the real k-axis

$$S_+(k)=\sqrt{S(k)}\mathrm{e}^{\mathrm{i}\vartheta},\quad S_-(k)=\sqrt{S(k)}\mathrm{e}^{-\mathrm{i}\vartheta}, \tag{61}$$

where $\vartheta(k)$ is a real function, $\vartheta(0)=0$. Thus,

$$L_+(k)=\frac{R_+}{H_+}S_+,\quad L_-(k)=\frac{R_-}{H_-}S_- \tag{62}$$

with

$$S_+(\mathrm{i}\infty)=S_-(-\mathrm{i}\infty)=L_+(\mathrm{i}\infty)=L_-(-\mathrm{i}\infty)=1. \tag{63}$$

It can also be checked that representation (62) defines the same asymptotes for $L_\pm(k)$ for $k\to 0$ $(V<1)$ as in (54)–(56).

This type of factorization will be used for the determination of waves with a non-zero wavenumber as well as for $V>1$. In spite of the fact that it contains an unknown phase ϑ, this representation is sufficient for the determination of the wave amplitudes. Note that it does not require the use of integral (52).

3.4. General homogeneous solution

Eq. (36) can now be expressed in the form

$$\frac{L_+}{2}p_+ + \frac{\mu}{L_-}u_- = -\frac{L_+(q_+ + q_-)}{2}+\frac{q_+ + q_-}{2L_-}. \tag{64}$$

In this equation, q_+ and q_- are considered as given external forces, and for the determination of two unknowns, p_+ and u_-, only one step remains: to represent the 'mixed' terms, L_+q_- and q_+/L_- as a sum of terms marked by '+' and '−' separately. For non-zero $q_\pm$ this can be done by the use of the Cauchy-type integral; however, in the following, we consider homogeneous solutions which correspond to $q(\eta)=0$ but with an energy flux from infinity.

If $q_+=q_-=0$ the right-hand side of Eq. (64) also is zero and homogeneous equation (64) has only the trivial solution $p_+=u_-=0$. Indeed, since the first (the second) term in the homogeneous equation has no singular points in the upper (lower) half-plane k including the real axis, their difference has no singular points in the whole of k-plane. Such a function (if it is not equal to zero) does not tend to zero when $k\to\infty$ and does not lead to any solution. Thus, the difference is zero as well as the sum, and $p_+=u_-=0$. This also follows directly from energy considerations. Indeed, the steady-state solution is considered as a limit, $t\to\infty$, $\eta=$ const, of a solution to the transient problem where no motion can arise under zero external forces.

To obtain a non-trivial solution of homogeneous Eq. (64), we have to admit an energy flux from infinity. For some 'resonant' values of k this can be done by considering non-zero q_+ or/and q_-, such that $q_\pm\to 0$ as $s\to 0$ and this is with a non-zero limit of the right-hand side of Eq. (64).

Consider wavenumber $k=h_{2v}$ $[1/L_+(h_{2v})=0]$ and external forces

$$q=C_{q-}\sqrt{2s}\exp[(s-\mathrm{i}h_{2v})\eta]H(-\eta),$$

$$q_-=C_{q-}\frac{\sqrt{2s}}{s+\mathrm{i}(k-h_{2v})},\quad q_+=0, \tag{65}$$

where $C_{q-}=\text{const}$, $s>0$. In a vicinity of $k=h_{2v}$

$$L_+\sim\frac{C_{2v}}{\sqrt{s-\mathrm{i}(k-h_{2v})}}, \tag{66}$$

where C_{2v} is a constant. We now get (see Appendix C)

$$\lim_{s\to+0}q=0,$$

$$\lim_{s\to 0}L_+q_-=C_{2v-}2\pi\delta(k-h_{2v})=C_{2v-}\left(\frac{1}{0+\mathrm{i}(k-h_{2v})}+\frac{1}{0-\mathrm{i}(k-h_{2v})}\right), \tag{67}$$

where $C_{2v-}=C_{q-}C_{2v}$. Similarly, if

$$q=C_{q+}\sqrt{2s}\exp[-(s-\mathrm{i}r_{2v-1})\eta]H(\eta),$$

$$q_+=C_{q+}\frac{\sqrt{2s}}{s-\mathrm{i}(k-r_{2v-1})},\quad q_-=0,$$

$$L_-\sim C_{2v-1}\sqrt{s+\mathrm{i}(k-r_{2v-1})} \tag{68}$$

then

$$\lim_{s\to+0} q = 0,$$

$$\lim_{s\to 0}\frac{q_+}{L_-} = C_{(2v-1)+}2\pi\delta(k-r_{2v-1}) = C_{(2v-1)+}\left(\frac{1}{0+\mathrm{i}(k-r_{2v-1})}+\frac{1}{0-\mathrm{i}(k-r_{2v-1})}\right), \tag{69}$$

where $C_{(2v-1)+} = C_{q+}C_{2v-1}$. At the same time, as shown in Appendix C

$$\lim_{s\to 0}\frac{q_-}{L_-} = \lim_{s\to 0} q_+L_+ = 0. \tag{70}$$

Using superposition we can thus represent Eq. (64) as

$$\frac{L_+}{2}p_+ + \frac{\mu}{L_-}u_- = \sum_{v=0}^{l} A_v\left(\frac{1}{0+\mathrm{i}(k-h_{2v})}+\frac{1}{0-\mathrm{i}(k-h_{2v})}\right) + \sum_{v=1}^{d+1} B_v\left(\frac{1}{0+\mathrm{i}(k-r_{2v-1})}+\frac{1}{0-\mathrm{i}(k-r_{2v-1})}\right) \quad (h_0=0) \tag{71}$$

whose solution is

$$p_+ = \frac{2}{L_+(k)}\left(\sum_{v=0}^{l}\frac{A_v}{0-\mathrm{i}(k-h_{2v})}+\sum_{v=1}^{d+1}\frac{B_v}{0-\mathrm{i}(k-r_{2v-1})}\right),$$

$$u_- = \frac{L_-(k)}{\mu}\left(\sum_{v=0}^{l}\frac{A_v}{0+\mathrm{i}(k-h_{2v})}+\sum_{v=1}^{d+1}\frac{B_v}{0+\mathrm{i}(k-r_{2v-1})}\right), \tag{72}$$

where A_v and B_v are arbitrary complex constants.

Solution (72) incorporates two types of waves: feeding waves and dissipative waves. The waves of the first type are associated with the explicitly shown singular points $k=r_{2v-1}$ in the expression for p_+ and points $k=h_{2v}$ $(v\neq 0)$ in the expression for u_-. They belong to the type which is characterized by an anomalous location of the wave relative to the crack front. To show this, consider a regular case where both functions h^2 and r^2 have only simple zeros, that is, there are no coincident zero points where $v_g = v$. In this case, the point $k=r_{2v-1}$ is not a singular or zero point of L_+ and the point $k=h_{2v}$ $(v\neq 0)$ is a regular point of L_-. So, these poles define constant-amplitude waves (denoted as $p=p_f$ and $u=u_f$)

$$p_f(\eta) = \frac{2}{L_+(r_{2v-1})}\sum_{v=1}^{d+1} B_v\exp(-\mathrm{i}r_{2v-1}\eta)H(\eta),$$

$$u_f(\eta) = \frac{L_-(h_{2v})}{\mu}\sum_{v=1}^{l} A_v\exp(-\mathrm{i}h_{2v}\eta)H(-\eta). \tag{73}$$

For $k\neq 0$ the group velocity, v_g, of the wave $k=r_{2v-1}$, which is located at the right, is less than its phase velocity, v, whereas $v_g > v$ for the wave $k=h_{2v}$ located at the left.

Since the group velocity is the energy flux velocity, these inequalities give evidence that each of these waves carries energy to the crack front. Such a wave can be called the *feeding* wave. Note that, under a given crack speed, not only one but several feeding waves can exist simultaneously. Some of them (with a wavenumber as r_{2v-1}) are placed ahead the crack front and others (with a wavenumber as h_{2v}) behind the front. Also note that these formulas (73) are written for the complex feeding waves associated with the positive zero points, $k = h_{2v}$ and $k = r_{2v-1}$. In addition, there are similar solutions for waves associated with points $k = -h_{2v}$ and $k = -r_{2v-1}$. In sum, these solutions represent real feeding waves (see the Conclusion).

In a particular case where two of the zeros coincide (in such a resonant point $v_g = v$), solutions (73) do not satisfy the reasonable requirement for the energy density to be finite. Indeed, in this latter case, the Fourier transform in a vicinity of the feeding wavenumber becomes [see (72)]

$$p_+ \sim \text{const}[0 - \mathrm{i}(k - r_{2v-1})]^{-3/2}, \quad \text{or} \quad u_- \sim \text{const}[0 + \mathrm{i}(k - h_{2v})]^{-3/2}, \tag{74}$$

and the amplitudes of the corresponding waves tend to infinity as $\sqrt{\pm\eta}$ ($\eta \to \pm\infty$), respectively. However, a dissipative wave associated with united zero points can exist. In this case, such singular points of h or r are separated in the solution: one of them belongs to p_+ (through L_+), while another belongs to u_- (through L_-).

Other waves of a non-zero wavenumber as a real singular point of $L_+(k)$ for $p(\eta)$ ($\eta > 0$) or $L_-(k)$ for $u(\eta)$ ($\eta < 0$) are located behind the crack front if $v_g < v$ and ahead the front if $v_g > v$. Thus they carry energy away from the crack front and can be called the *dissipative* waves.

In the case of a zero wavenumber, the group and phase velocities coincide but in this case the steady-state formulation of the problem does not exclude the possibility for the crack speed to be different from the wave speed.

3.5. Classical macrolevel solution

The classical solution valid for a homogeneous medium can be obtained as a long-wave asymptote ($k \to 0$) of the macrolevel-associated solution extended then all over the spectrum. To find this asymptote one has to return to the initial definition of the variable η as $x - vt$ [in contrast to (22)] and to substitute ak instead k in the above relations. Also, we denote $p_+ = a\sigma_+$, where σ is stress. In this way, one can find that in solution (72) with σ_+ instead p_+

$$L = \frac{2}{k^2 + (0 + \mathrm{i}kV)^2}, \quad l = 0, \quad B_v = 0. \tag{75}$$

For $0 \le V < 1$ this leads to

$$\begin{aligned} L_\pm &= \sqrt{2}(1 - V^2)^{-1/4}(0 \mp \mathrm{i}k)^{-1/2}, \\ \sigma_+(k) &= \sqrt{2}A_0(1 - V^2)^{1/4}(0 - \mathrm{i}k)^{-1/2}, \\ u_-(k) &= \frac{\sqrt{2}A_0}{\mu}(1 - V^2)^{-1/4}(0 + \mathrm{i}k)^{-3/2}. \end{aligned} \tag{76}$$

The constant A_0 can be expressed in terms of the energy release rate G. From the known formula

$$G = \lim_{s\to\infty} s^2\sigma_+(\mathrm{i}s)u_-(-\mathrm{i}s) \tag{77}$$

it follows that $A_0 = \sqrt{\mu G/2}$ and

$$\sigma_+(k) = \sqrt{\mu G}(1-V^2)^{1/4}(2(0-\mathrm{i}k))^{-1/2},\ u_-(k) = \frac{\sqrt{G}}{\mu}(1-V^2)^{-1/4}(0+\mathrm{i}k)^{-3/2},$$
$$\sigma(\eta) = (1-V^2)^{1/4}\sqrt{\frac{\mu G}{\pi\eta}}H(\eta),\ u(\eta) = 2(1-V^2)^{-1/4}\sqrt{\frac{-G\eta}{\pi\mu}}. \tag{78}$$

This solution is the same as the well-known solution following directly from the dynamic equation for the corresponding homogeneous medium. Letting $G=\mathrm{const}\sqrt{1-V^2}$ one can see that this solution is valid for $V=1$ as well (in this case, $G=0$). However, for $V=1$ the zero-energy-release solution is not unique. As follows directly from the dynamic equation, any solution where $u(\eta)$ is an arbitrary function equal to zero for $\eta>0$, is valid as the d'Alembert solution.

For $V>1$ the functions $L_\pm$ can be represented as

$$L_+(k) = 1, \quad L_-(k) = \frac{2}{\sqrt{V^2-1}(0+\mathrm{i}k)} \tag{79}$$

and it can be seen that neither A_v nor B_v terms on the right-hand side of (72) can appear [see (67) and (69)]. This means that no supersonic crack can exist in the framework of the homogeneous-material model. Note, however, that a zero-energy-release supersonic solution exists in the case of a non-homogeneous problem.

3.6. Macrolevel-associated solution

Consider now an A_0-associated solution of (72), that is, a solution which owes its origin to a zero-wavenumber feeding wave ($h_0=0$). A long-wave approximation of this solution coincides with the macrolevel solution (78). This is a distinguishing feature of the macrolevel-associated solution.

The internal force in a bond at the moment preceding its disintegration, $\eta=+0$, can be found using the limiting theorem (A.9) cited in Appendix A

$$p(+0) = \lim_{s\to\infty} sp_+(\mathrm{i}s). \tag{80}$$

3.6.1. Subsonic crack propagation

Using relations (72) and (54), we find the internal force, displacement and local energy release rate as

$$p(+0) = 2A_0, \quad u(-0) = u(+0) = \frac{A_0}{\mu}, \quad G_0 = p(+0)u(0) = \frac{2A_0^2}{\mu}. \tag{81}$$

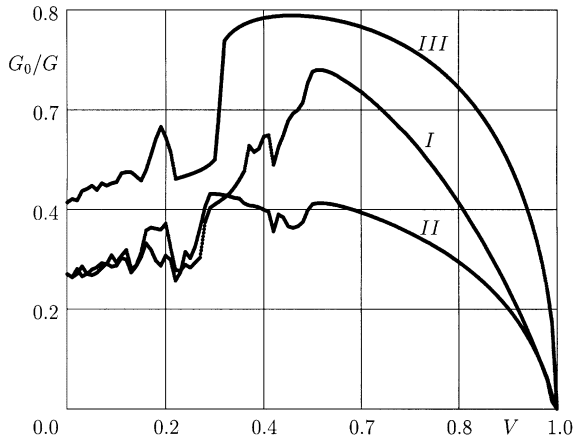

Fig. 6. Energy release ratios, G_0/G, for fracture modes I–III.

The global energy release rate is defined by the long-wave asymptotes of $L_{\pm}$ (54). Using (72) and (77) we obtain

$$G = \frac{2A_0^2}{\mu}\mathscr{R}^{-2}. \tag{82}$$

Thus, the total resistance to the crack propagation can be expressed as follows:

$$G = G_0\mathscr{R}^{-2} = G_0 \exp\left(-\frac{2}{\pi}\int_0^{\infty} \frac{\operatorname{Arg} L(\xi)}{\xi}\,\mathrm{d}\xi\right)$$

$$= G_0 \prod_{v=1}^{d+1} r_{2v-1} \prod_{v=1}^{l} h_{2v} \left(\prod_{v=1}^{d} r_{2v} \prod_{v=1}^{l+1} h_{2v-1}\right)^{-1}. \tag{83}$$

The difference $G - G_0$ represents the wave resistance to the crack propagation. The energy release ratio, G_0/G, as a function of the normalized crack speed is shown in Fig. 6 for three fracture modes (for modes I and II it is the ratio of the crack speed to the Rayleigh wave speed). These results were first obtained in Slepyan (1981a) and Kulakhmetova et al. (1984).

Note that only two zero points remain in the expression for $\mathscr{R}$ (55) when $v \to c$, namely

$$\mathscr{R} = \sqrt{\frac{h_1}{r_1}}, \quad \lim r_1 \approx 2.809, \quad h_1 \sim \sqrt{12(1-V^2)}. \tag{84}$$

As $V \to 1$, $h_1 \to 0$ and if $G_0 \neq 0$ the global resistance $G \to \infty$. However, letting $A_0/\mathscr{R} = \text{const}$, we obtain a finite global resistance under the vanishing local energy release rate.

3.6.2. Supersonic crack propagation

In the case $V > 1$, the functions $L_{\pm}(k)$ can be represented as [see (59)–(63)]

$$L_+(k) = S_+(k) \sim \sqrt{\frac{2}{r_1\sqrt{V^2-1}}} \quad (k \to 0),$$

$$L_-(k) = \sqrt{1+\left(\frac{r_1}{0+\mathrm{i}k}\right)^2}\,S_- \sim \sqrt{\frac{2r_1}{\sqrt{V^2-1}}}\,\frac{1}{0+\mathrm{i}k} \quad (k \to 0), \tag{85}$$

where r_1 satisfies the equation

$$6 - 2\cos r_1 - V^2 r_1^2 = 0. \tag{86}$$

From this, it follows that $L_+(0) > 1$. Indeed,

$$r_1^2(V^2-1) = 4 - r_1^2 + 2(1-\cos r_1) < 4. \tag{87}$$

The solution is [see (72)]

$$p_+ = \frac{2B_1}{(0-\mathrm{i}k)L_+}, \quad u_- = \frac{B_1 L_-}{\mu(0+\mathrm{i}k)} \tag{88}$$

with the asymptotes

$$p_+ \sim \frac{2B_1}{L_+(0)(0-\mathrm{i}k)}, \quad u_- = \frac{2B_1}{\mu\sqrt{V^2-1}\,L_+(0)(0+\mathrm{i}k)^2} \quad (k \to 0),$$

$$p_+ \to \frac{2B_1}{0-\mathrm{i}k} \ (k \to \mathrm{i}\infty), \quad u_- \to \frac{B_1}{\mu(0+\mathrm{i}k)} \ (k \to -\mathrm{i}\infty). \tag{89}$$

The corresponding originals are

$$p(\eta) \sim \frac{2B_1}{L_+(0)} \ (\eta \to \infty), \quad u_- = -\frac{2B_1\eta}{\mu\sqrt{V^2-1}L_+(0)} \ (\eta \to -\infty),$$

$$p_+ = 2B_1 \ (\eta = +0), \quad u_- = \frac{B_1}{\mu} \ (\eta = 0) \tag{90}$$

or, denoting $(2B_1)/L_+(0) = p_0$

$$p(\eta) \sim p_0 \ (\eta \to \infty), \quad u_- = -\frac{p_0\eta}{\mu\sqrt{V^2-1}} \ (\eta \to -\infty),$$

$$p(+0) = p_0 L_+(0), \quad u_-(0) = \frac{p_0 L_+(0)}{2\mu}. \tag{91}$$

This solution corresponds to supersonic crack propagation in a lattice under an initially uniform stress field: p_0 is the initial internal force in the bonds normal to the crack. In contrast to the macrolevel classical solution, the supersonic macrolevel-associated solution exists and shows a nonzero local energy release rate. What is more, the internal force in the breaking bond exceeds the initial value: $p(+0)/p_0 = L_+(0) > 1$. This involves the possibility of crack propagation under a load uniformly distributed along

the crack surfaces in an initially unstressed lattice. The supersonic propagation can take place under the condition

$$L_+(0)p_0 = p_c, \tag{92}$$

where $L_+(0)$ is defined by (85) and p_c is a critical force.

Thus, relative to the homogeneous material model, the lattice model decreases the local energy release rate in the case of subsonic crack propagation and increases it (from zero to a positive value) in the supersonic case. The latter phenomenon, which reflects itself in the inequality $L_+(0) > 1$, arises due to the fact that the zone of influence of the shear wave in the lattice stretches ahead of its quasi-front propagating with speed c.

3.7. Microlevel solutions

We now use general solution (72) to find solutions associated with a nonzero feeding wavenumber. In the considerations below, we refer to some relations derived in Appendix D.

3.7.1. Subsonic crack under the feeding wave with $v_g > v$

In this case, the feeding wave is represented by the formula for u_f in (73). Referring to (61) and (62), we get the following expression for the feeding wave:

$$u_f(\eta) = \frac{A_v}{\mu}\frac{R_-(h_{2v})}{H_-(h_{2v})}\sqrt{S(h_{2v})}\exp[-\mathrm{i}(h_{2v}\eta + \vartheta)]H(-\eta), \tag{93}$$

where an expression for S is given by (D.3) and $\vartheta = \vartheta(h_{2v})$ is a real constant.

As to the contribution of the same point, $k = h_{2v}$, to $p(\eta)$, we consider an asymptote of it for $\eta \to \infty$ which is defined by an asymptote of p_+ for $k \to h_{2v}$. The latter asymptote is [see (72)]

$$p_+ \sim \frac{A_v P_1}{\sqrt{0 - \mathrm{i}(k - h_{2v})}},$$

$$P_1 = \frac{2}{R_+(h_{2v})\sqrt{S(h_{2v})}}\sqrt{\frac{2}{h_{2v}}\prod_{\mu\neq v}^{l}\left[1 + \left(\frac{h_{2\mu}}{0 - \mathrm{i}h_{2v}}\right)^2\right]}\exp[\mathrm{i}(\pi/4 - \vartheta)] \tag{94}$$

and

$$p(\eta) \sim \frac{A_v P_1}{\sqrt{\pi\eta}}\exp(-\mathrm{i}h_{2v}\eta)H(\eta), \tag{95}$$

It is a dissipative wave (its trace on the x-axis) of the same wavenumber as the feeding wave.

Note that such a solution does not exist for $V > V_0 \approx 0.2172$ where $l = 0$ and there are no waves with $v_g > v$.

3.7.2. Sub- and supersonic cracks under the feeding wave with $v_g < v$

Now consider the first formula in (73) which corresponds to the inequality $v_g < v$. The feeding wave at $\eta > 0$ is

$$p(\eta) = \frac{2B_v H_+(r_{2v-1})}{R_+(r_{2v-1})\sqrt{S(r_{2v-1})}} \exp[-\mathrm{i}(r_{2v-1}\eta + \vartheta)] H(\eta), \tag{96}$$

where an expression for S is given by (D.5) and $\vartheta = \vartheta(r_{2v-1})$.

The dissipative wave of the same wavenumber is defined by (72) as

$$u_- \sim \frac{B_v U_1}{\sqrt{0 + \mathrm{i}(k - r_{2v-1})}},$$

$$U_1 = \frac{\sqrt{S(r_{2v-1})}}{\mu H_-(r_{2v-1})} \sqrt{\frac{2}{r_{2v-1}} \prod_{\mu \neq v}^{d+1} \left[1 + \left(\frac{r_{2\mu-1}}{0 - \mathrm{i}r_{2v-1}}\right)^2\right]} \exp[-\mathrm{i}(\pi/4 + \vartheta)] \tag{97}$$

and

$$u(\eta) \sim \frac{B_v U_1}{\sqrt{-\pi\eta}} \exp(-\mathrm{i}h_{2v}\eta) H(-\eta). \tag{98}$$

Let us now consider the case $V > V_1$ in detail. In this case, $l = d = 0$, the feeding wavenumber is r_1 and if $V \leq 1$

$$R_-(k) \sim \sqrt{1 + \left(\frac{r_1}{0 + \mathrm{i}k}\right)^2},$$

$$R_+(r_1) = H_+(r_1) = 1, \quad H_-(r_1) = \sqrt{1 - \frac{h_1^2}{r_1^2}},$$

$$S_\pm(r_1) = \left[\frac{V^2 r_1^2 - r_1 \sin r_1}{4}\left(1 - \frac{h_1^2}{r_1^2}\right)\right]^{1/4} \mathrm{e}^{\pm \mathrm{i}\vartheta}. \tag{99}$$

These relations with $h_1 = 0$ are still valid for $V \geq 1$ as well [see (59)]. We now find

$$p_f(\eta) = 2B_1 \left[\frac{V^2 r_1^2 - r_1 \sin r_1}{4}\left(1 - \frac{h_1^2}{r_1^2}\right)\right]^{-1/4} \exp[-\mathrm{i}(r_1\eta + \vartheta)]$$
$$(h_1 = 0 \text{ for } V \geq 1). \tag{100}$$

Note that

$$p(\eta) \sim p_f(\eta) \ (\eta \to \infty), \quad p(+0) = 2B_1. \tag{101}$$

It follows that

$$\frac{p(+0)}{|p(\infty)|} = \left[\frac{V^2 r_1^2 - r_1 \sin r_1}{4}\left(1 - \frac{h_1^2}{r_1^2}\right)\right]^{1/4}, \tag{102}$$

where $h_1 = 0$ for $V \geq 1$. This ratio exceeds unity if $V > V^* \approx 0.50$. Otherwise the limiting value of the internal force is achieved ahead the crack front, and hence the solution

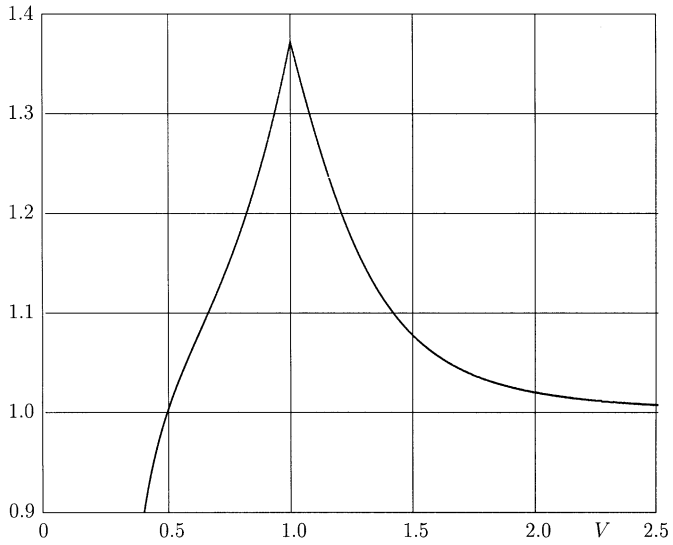

Fig. 7. Ratio $p(0)/p(\infty)$ for the feeding wavenumber equal to r_1 ($l = d = 0$).

is not valid for $V < V^*$. The ratio as a function of the crack speed is represented in Fig. 7.

In this process, the energy flux velocity relative to the propagating crack front is directed backwards. In other words, the crack propagating faster absorbs energy from the wave. Such a phenomenon, that of an energy absorber trailing along at the back of the wave, can exist independently of whether the system is discrete or continuous, with the existence of a wave with $v_g < v$ being the condition. In this connection, we refer to the above considered simple example as a string on an elastic foundation under a moving load.

As to the crack opening displacement, it decreases asymptotically as $1/\sqrt{-\eta}$ ($\eta \to -\infty$). In the same way, it can be found that

$$u(\eta) \sim \frac{B_1}{\mu}\sqrt{\frac{1}{\pi r_1}}\left[\frac{V^2 r_1^2 - r_1 \sin r_1}{1 - h_1^2/r_1^2}\right]^{-1/4} \frac{H(-\eta)}{\sqrt{-\eta}} \exp[-\mathrm{i}(r_1\eta + \pi/4 + \vartheta)]. \quad (103)$$

This is a dissipative wave propagating behind the crack front.

3.8. Other dissipative waves

An asymptote of a dissipative wave on the line $y = 0$ ($n = 0$) can be determined in an explicit form. Consider a solution contained in (72)

$$p_+ = \frac{2H_+}{R_+ S_+}\frac{C}{0 - \mathrm{i}(k - k_\mathrm{f})}, \quad u_- = \frac{R_- S_-}{\mu H_-}\frac{C}{0 + \mathrm{i}(k - k_\mathrm{f})}, \quad (104)$$

where C is a constant and k_f is the feeding wavenumber (the feeding wave delivers energy to the crack front from the right if $k_\mathrm{f} = r_{2\nu-1}$ and from the left if $k_\mathrm{f} = h_{2\nu}$).

Each real branch point of these expressions defines a dissipative wave carrying energy away from the crack front. The contribution, $\mathscr{C}_1(\eta)\mathrm{e}^{-\mathrm{i}k_*\eta}$, of a branch point of type $[0 \pm \mathrm{i}(k-k_*)]^{-1/2}$, where k_* is a real constant, for $\eta \to \mp\infty$ is defined by the Fourier transform in an arbitrary small vicinity of this point. Another type, $[0 \pm \mathrm{i}(k-k_*)]^{1/2}$, gives a contribution, $\mathscr{C}_2(\eta)\mathrm{e}^{-\mathrm{i}k_*\eta}$ which can be determined using the equality as

$$\mathscr{C}_2(\eta) = \mp\frac{\mathrm{d}\mathscr{C}_2(\eta)}{\mathrm{d}\eta}. \tag{105}$$

We consider here waves with $k_* \neq \pm k_\mathrm{f}$ (the opposite case was just considered). As can be seen the dissipative wave is placed ahead (behind) the crack front if k_* is a singular point of H_+ or R_+ (H_- or R_-), that is, $k_* = h_{2v}$ or $k_* = r_{2v}$ ($k_* = h_{2v-1}$ or $k_* = r_{2v-1}$). Further, as follows from (104) and (105) these waves decrease with the distance from the crack front as $|\eta|^{-1/2}$ ('slowly decreasing' wave) or $|\eta|^{-3/2}$ ('fast-decreasing' wave), namely

$$p_+ \sim \mathrm{const}\sqrt{0-\mathrm{i}(k-k_*)}, \quad p \sim \frac{\mathrm{const}}{\eta^{3/2}}\mathrm{e}^{-\mathrm{i}k_*\eta}, \ (k_* = h_{2v}, \ \eta \to \infty),$$

$$p_+ \sim \frac{\mathrm{const}}{\sqrt{0-\mathrm{i}(k-k_*)}}, \quad p \sim \frac{\mathrm{const}}{\eta^{1/2}}\mathrm{e}^{-\mathrm{i}k_*\eta}, \ (k_* = r_{2v}, \ \eta \to \infty),$$

$$u_- \sim \frac{\mathrm{const}}{\sqrt{0+\mathrm{i}(k-k_*)}}, \quad u \sim \frac{\mathrm{const}}{(-\eta)^{1/2}}\mathrm{e}^{-\mathrm{i}k_*\eta}, \ (k_* = h_{2v-1}, \ \eta \to -\infty),$$

$$u_- \sim \mathrm{const}\sqrt{0+\mathrm{i}(k-k_*)}, \quad u \sim \frac{\mathrm{const}}{(-\eta)^{3/2}}\mathrm{e}^{-\mathrm{i}k_*\eta}, \ (k_* = r_{2v-1}, \ \eta \to -\infty). \tag{106}$$

These expressions are still valid for the particular case where two zeros unite. In this case, there are two waves, one is ahead and another behind the crack front with different exponents in their asymptotic dependences of η.

Note that the total dissipation corresponding to the macrolevel-associated solution is defined by (83). Also note that the 'fast-decreasing' wave is found here only for the crack surface and its continuation, $y = n = 0$. Waves in the x, y-plane are considered below.

3.9. Structure of the waves in the x, y-plane

3.9.1. The carrier wave modes

Consider wave modes associated with the singular points of the functions h and r. For $k = h_v$, where $h = 0$, as follows from (29)

$$\lambda = 1, \quad u_n = u_0. \tag{107}$$

Note that these equalities are considered under the condition $s = 0$. Thus, the carrier wave is independent of n and

$$u = \exp(-\mathrm{i}h_v\eta). \tag{108}$$

In contrast, if $k = r_v$ $(r = 0)$

$$\lambda = -1, \quad u_{n+1} = -u_n \tag{109}$$

and

$$u = (-1)^n \exp(-\mathrm{i} r_v \eta). \tag{110}$$

This means antiphase oscillations of the neighboring particles (particle n, m and particle $n+1, m$).

The existence of these wave modes in the lattice also follows directly from its dynamic Eq. (25). Indeed, if $u^{\mathrm{F}}_{n+1} = u^{\mathrm{F}}_{n-1} = u^{\mathrm{F}}_n$ $(\lambda = 1)$ then $h^2 = 0$, while if $u^{\mathrm{F}}_{n+1} = u^{\mathrm{F}}_{n-1} = -u^{\mathrm{F}}_n$ $(\lambda = -1)$ then $h^2 + 4 \equiv r^2 = 0$. Dispersion relations of these two modes are shown in Fig. 5.

3.9.2. Group velocity as a vector

Let us now return to Eq. (21). In terms of the non-dimensional variables adopted in this section, $x' = x/a$, $y' = y/a$, $t' = ct/a$ $(V = v/c)$, with the superscript dropped, this equation is

$$\frac{\mathrm{d}^2 u(x,y)}{dt^2} = u(x+1,y) + u(x-1,y) + u(x,y+1) + u(x,y-1) - 4u(x,y). \tag{111}$$

Substituting a solution as a wave

$$u = \exp[\mathrm{i}(\Omega t - kx - py)], \tag{112}$$

one obtains the dispersion relation

$$\Omega^2 = 4 - 2\cos k - 2\cos p \tag{113}$$

which defines the following projections of the phase and group velocities onto the x and y axes:

$$V = (\mathbf{V})_x = \frac{\Omega}{k}, \quad (\mathbf{V}_{\mathrm{g}})_x = \frac{\partial \Omega}{\partial k} = \frac{\sin k}{\Omega},$$
$$(\mathbf{V})_y = \frac{\Omega}{p}, \quad (\mathbf{V}_{\mathrm{g}})_y = \frac{\partial \Omega}{\partial p} = \frac{\sin p}{\Omega}. \tag{114}$$

Now consider the above-determined wave modes. Let Ω be non-zero. For $k = h_v$, that is, for $h^2 = 2(1 - \cos k) - \Omega^2 = 0$, it follows from (113) that $\cos p = 1$ and hence $(\mathbf{V}_{\mathrm{g}})_y = 0$. The same result is valid for $k = r_v$. Indeed, if $r^2 = 6 - 2\cos k - \Omega^2 = 0$ it follows that $\cos p = -1$ and hence $\sin p = 0$ as in the previous case. Thus the group velocities of the considered waves are parallel to x-axis. This, however, does not mean that the energy of dissipative waves remains on the lines $n = 0$ and $n = -1$. The fact is that each of such waves is formed by a group of waves associated with a vicinity of the corresponding branch point of the Fourier transform, while the group velocities determined here are valid only for a sinusoidal wave with the singular-point wavenumber.

3.9.3. Wave amplitude in the x, y-plane

3.9.4. Feeding wave with $v_g > v$

Consider the feeding wave associated with the coefficient A_v in (72). On the line $n = 0$, the displacement is defined as follows:

$$u_0^F(k) = u_+ + u_-,$$
$$u_+ = \frac{p_+}{2\mu} = \frac{A_v}{\mu L_+(k)[0 - \mathrm{i}(k - h_{2v})]}, \quad u_- = \frac{A_v L_-(k)}{\mu[0 + \mathrm{i}(k - h_{2v})]}. \tag{115}$$

Referring to (28) and (29) the displacement for any $n \geq 0$ can be expressed as

$$u_n(\eta) = u_n^+(\eta) + u_n^-(\eta),$$
$$u_n^\pm(\eta) = \frac{1}{2\pi}\int_{-\infty}^{\infty} u_\pm(k)\lambda^n \mathrm{e}^{-\mathrm{i}k\eta}\,\mathrm{d}k, \quad \lambda = \frac{r-h}{r+h}. \tag{116}$$

A contribution of the point $k = h_{2v}$ for $\eta < 0$ is defined by u_n^- as a residue at this point where $h = 0$. Indeed, the pole of u_- is $k = h_{2v} + \mathrm{i}0$, while as shown in Appendix D [see (D.3) and (D.4)], the corresponding branch point of λ is $k = h_{2v} - \mathrm{i}0$ and hence it gives no contribution for $\eta < 0$. As a result, taking symmetry of the solution into account, we have

$$u_n(\eta) = -u_{-n-1}(\eta) = \frac{L_-(h_{2v})}{\mu} A_v \exp(-\mathrm{i}h_{2v}\eta) \quad (n = 0, 1, \ldots). \tag{117}$$

Another term, u_n^+, gives no contribution of this point for $\eta < 0$ since the corresponding branch points of u_+ and λ are below the real axis of the k-plane, while the contour of integration can be transformed upward (to $+\infty$).

Now consider this wave at $\eta > 0$ ($n \geq 0$). In this case, both terms are to be taken into account, and we find an asymptote of $u_n(\eta)$ for $n \geq 0$, $\zeta = \sqrt{\eta^2 + n^4} \to \infty$. This asymptote can be derived from the integral (116) as

$$u_n^\pm(\eta) \sim \frac{1}{2\pi}\int_{h_{2v}-\varepsilon}^{h_{2v}+\varepsilon} u_\pm(k)\exp(-nh - \mathrm{i}k\eta)\,\mathrm{d}k, \tag{118}$$

where the asymptote of λ ($k \to h_{2v}$) (D.4) is used and ε is any small positive number. Substituting $k = h_{2v} + k'/\zeta$ (the superscript is dropped below) one obtains

$$u_n^-(\eta) \sim \frac{A_v L_-(h_{2v})}{2\pi\mu}\int_{-\varepsilon\zeta}^{\varepsilon\zeta} \exp[-h^0\beta(1+\beta^4)^{-1/4}\sqrt{k + \mathrm{i}0}$$
$$-\mathrm{i}(1+\beta^4)^{-1/2}k]\frac{\mathrm{d}k}{0 + \mathrm{i}k}\exp(-\mathrm{i}h_{2v}\eta),$$
$$h^0 = \sqrt{2h_{2v}V(V_g - V)}, \quad \beta = n/\sqrt{\eta}, \tag{119}$$

where the asymptotic expression for $h(k)$ (D.3) is used. In this expression, since $\zeta \to \infty$, limits of integration can be displaced by $\mp\infty$. After this a substitution

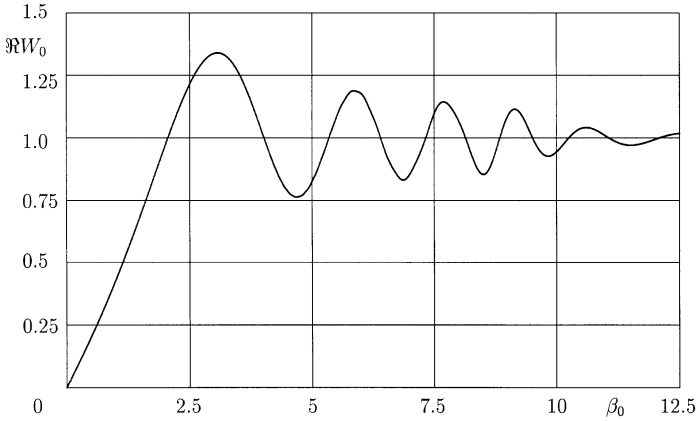

Fig. 8. Real part of the function (121) for the feeding wave under the knife-edge diffraction.

$k = k''\sqrt{1+\beta^4}$ leads to

$$u_n^-(\eta) \sim W\exp(-\mathrm{i}h_{2v}\eta)$$
$$W = \frac{A_v L_-(h_{2v})}{2\mu}\left\{1 - \frac{\mathrm{i}}{\pi}\int_0^\infty [\exp(-h^0\beta\sqrt{k} - \mathrm{i}k) - \exp(-\mathrm{i}h^0\beta\sqrt{k} + \mathrm{i}k)]\frac{\mathrm{d}k}{k}\right\}. \tag{120}$$

By means of a transformation of the integral contour for the first term (rotate the ray, $+0, \infty$, clockwise to the negative half-axis and then change k to $-k^2$), the amplitude, W, can also be represented as

$$W = \frac{A_v L_-(h_{2v})}{\mu} W_0(\beta_0), \quad \beta_0 = h^0\beta,$$
$$W_0(\beta_0) = \frac{2}{\pi}\int_0^\infty \exp(\mathrm{i}k^2)\sin(\beta_0 k)\frac{\mathrm{d}k}{k}. \tag{121}$$

It can be easily seen that the amplitude as a function of β_0 is equal to zero for $\beta_0 = 0$ ($n = 0$), as it should (since $u_0^- = u_-$), and becomes the same as for $\eta < 0$ (117) if $\beta_0 = h^0 n/\sqrt{\eta} \gg 1$. The function $\Re W_0(\beta_0)$ is shown in Fig. 8.

Thus, for $\eta \leq 0$, the feeding wave (117), (120), (121) consists of two one-dimensional n-independent waves propagating separately in the upper, $n \geq 0$, and lower, $n \leq -1$, half-planes. These waves, however, meet a moving obstacle at $\eta \geq 0$ in the form of intact bonds on the crack continuation. As a result, a special 'knife-edge' diffraction arises where the feeding wave loses energy by disintegration of the bonds and excitation of the dissipative waves. This leads to the relaxation of the wave in a vicinity of the crack continuation as reflected by the derived solutions. Note that the feeding wave itself does not reflect from this obstacle, however, it gives rise to the dissipative waves one of which is just considered and others are represented as contributions of other singular points of the Fourier transform (115).

3.9.5. 'Slowly decreasing' dissipative wave

We now have to consider the second term, u^+ (115), which corresponds to a dissipative wave. In contrast to u_-, which has a simple pole at $k = h_{2v}$, the function u_+ has a square-root type branch point [see (94)]:

$$u_+(k) \sim \frac{A_v P_1}{2\mu\sqrt{0 - \mathrm{i}(k - h_{2v})}}. \tag{122}$$

In this case, a contribution of a stationary point must be taken into account. In this connection, consider the function $\lambda(k)$. For $h_{2v-1} < k < h_{2v}$, where $h(k) = i|h(k)|$, $r > 0$, it can be expressed as

$$\lambda = \mathrm{e}^{-\mathrm{i}g(k)}, \quad g(k) = 2\arctan\frac{|h(k)|}{r(k)} \tag{123}$$

with derivative $\mathrm{d}g/\mathrm{d}k$ varying from $+\infty$ ($k = h_{2v-1} + 0$) to $-\infty$ ($k = h_{2v} - 0$). Hence, a stationary point, $k = k_0$, exists in this segment for the phase $\mathscr{P} = -ng(k) - k\eta$ in the expression

$$u_n^+(\eta) = \frac{1}{2\pi}\int u_+(k)\lambda^n \exp(-\mathrm{i}k\eta)\,\mathrm{d}k \tag{124}$$

with the integration in a vicinity of the point $k = h_{2v}$, such that

$$\frac{\mathrm{d}\mathscr{P}}{\mathrm{d}k} = n\frac{\mathrm{d}g}{\mathrm{d}k} + \eta = 0. \tag{125}$$

The singular point of $u_+(k)$ can be removed from the integrand by substitutions $k = h_{2v} \pm l^2$ for $k > h_{2v}$ and $k < h_{2v}$, respectively. The stationary point, l_0, and the phase become

$$\begin{aligned} l_0 &= \sqrt{h_{2v} - k_0}, \\ \mathscr{P}(l) &= -ng(h_{2v} - l^2) + l^2\eta - \mathrm{i}h_{2v}\eta, \\ \frac{\mathrm{d}\mathscr{P}}{\mathrm{d}l} &= -ng' + 2l\eta, \\ \frac{\mathrm{d}^2\mathscr{P}}{\mathrm{d}l^2} &= -ng'' + 2\eta, \\ g' &= \frac{\mathrm{d}g}{\mathrm{d}l}, \quad g'' = \frac{\mathrm{d}^2 g}{\mathrm{d}l^2}, \quad -ng'(h_{2v} - l_0^2) + 2l_0\eta = 0. \end{aligned} \tag{126}$$

As a result, for $\zeta \to \infty$, integral (124) can be represented as

$$\begin{aligned} u_n^+(\eta)\exp(\mathrm{i}h_{2v}\eta) \sim \frac{1}{\pi}\int_0^p & l u_+ \exp[-\mathrm{i}ng(h_{2v} - l^2) + \mathrm{i}l^2\eta)\,\mathrm{d}l \\ & + \frac{A_v P_1}{2\pi\mu}\int_0^\varepsilon \exp(-h^0 nl - \mathrm{i}l^2\eta + \mathrm{i}\pi/4)\,\mathrm{d}l, \end{aligned} \tag{127}$$

where p is a number ($\sqrt{h_{2\nu}-l_0}<p<\sqrt{h_{2\nu}-h_{2\nu-1}}$) and ε is an arbitrary small positive constant. From this it follows that

$$u_n^+(\eta)\sim\frac{\sqrt{l_0}u_+}{\sqrt{\pi(|2\eta-ng''|)}}\exp[\mathrm{i}(l_0^2\eta-ng-h_{2\nu}\eta)]$$
$$+\frac{A_\nu P_1}{2\pi\mu\sqrt{\eta}}\int_{-\beta_0/2}^{\infty}\exp(\mathrm{i}l^2)\,\mathrm{d}\,l\exp[-\mathrm{i}(\beta_0^2/4+h_{2\nu}\eta-\pi/4)]\quad(l=l_0). \tag{128}$$

This result is valid for a non-zero ratio n/η. In the case $n/\eta\to 0$, the stationary point, l_0, also tends to zero. In this case, the asymptotes of u_+ and λ ($k\to h_{2\nu}$) can be used in the first term of the above representation (128) as well as in the second one and a multiplier as $1/2$ must be introduced in the first term. We obtain

$$u_n^+(\eta)\sim\frac{A_\nu P_1}{\pi\mu\sqrt{\eta}}\int_0^{\infty}\exp(\mathrm{i}l^2)\cos\beta_0 l\,\mathrm{d}l\exp[-\mathrm{i}(h_{2\nu}\eta+\pi/4)]$$
$$=\frac{A_\nu P_1}{2\mu\sqrt{\pi\eta}}\exp[-\mathrm{i}(\beta_0^2/4+h_{2\nu}\eta)], \tag{129}$$

where P_1 is defined in (94).

Note that in this case, $n/\eta\ll 1$, the initial representation of wave (124) takes the form

$$u_n^+(\eta)=\frac{1}{2\pi}\int_{-\varepsilon}^{\varepsilon}u_+(k)\exp(-nh(k)-\mathrm{i}k\eta)\,\mathrm{d}k \tag{130}$$

and this leads to (129).

3.9.6. Feeding wave with $v_g<v$ and the associated dissipative wave

Similarly, in the case of B_ν-associated feeding wave, the Fourier transform of the displacement field for $n\geq 0$ is

$$u_n^{\mathrm{F}}(k)=u_0^{\mathrm{F}}(k)\lambda^n,\quad u_0^{\mathrm{F}}(k)=u_+ +u_-,$$
$$u_+=\frac{p_+}{2\mu}=\frac{B_\nu}{\mu L_+(k)[0-\mathrm{i}(k-r_{2\nu-1})]},\quad u_-=\frac{B_\nu L_-(k)}{\mu[0+\mathrm{i}(k-r_{2\nu-1})]}. \tag{131}$$

A contribution of point $k=r_{2\nu-1}$ for $\eta>0$ is defined by u_n^+ as a residue at this point [in the inverse transformation as in (116)] where $r=0$, while u_n^- gives no contribution at $\eta>0$. Due to symmetry, the displacement field is

$$u_n(\eta)=\frac{B_\nu}{\mu L_+(r_{2\nu-1})}(-1)^n\exp(-\mathrm{i}r_{2\nu-1}\eta)\quad(n=0,\pm1,\ldots). \tag{132}$$

For $\eta<0$ each term gives a contribution. By similar considerations as above, one can conclude: The feeding wave corresponding to the first term, u_n^+, is

$$u_n(\eta)\sim\frac{B_\nu}{\mu L_+(r_{2\nu-1})}\overline{W_0(\gamma_0)}(-1)^n\exp(-\mathrm{i}r_{2\nu-1}\eta)\quad(n=0,\pm1,\ldots), \tag{133}$$

$$\gamma_0=r^0 n/\sqrt{-\eta},\quad r^0=\sqrt{2r_{2\nu-1}V(V-V_{\mathrm{g}})}\quad(\zeta\to\infty), \tag{134}$$

where W_0 is defined in (121).

In this case, the knife-edge diffraction is caused by the free surfaces of the crack. Their influence and the energy loss by disintegration of the bonds and excitation of the dissipative waves lead to the relaxation of the wave in a vicinity of the crack surfaces at $\eta < 0$, as reflected by (133).

The associated dissipative wave corresponding to the second term, u_n^-, can be found using considerations similar to those used in the case $v_g > v$. In particular, for $n/|\eta| \ll 1$ ($\eta \to -\infty$) the displacements are

$$u_n(\eta) \sim \frac{2B_v U_1}{\pi\sqrt{-\eta}}(-1)^n \int_0^\infty \exp(\mathrm{i}k^2)\cos\gamma_0 k\,\mathrm{d}k \exp(-\mathrm{i}r_{2v-1}\eta - \mathrm{i}\pi/4)$$

$$= \frac{B_v U_1}{\sqrt{-\pi\eta}}(-1)^n \exp[-\mathrm{i}(\gamma_0^2/4 + r_{2v-1}\eta], \tag{135}$$

where U_1 is defined in (97).

3.9.7. 'Fast-decreasing' dissipative wave

Consider a contribution of the branch point, $k = h_{2v}$, of the expression for u_+ (131). For $n/\eta \ll 1$ the use of an asymptote ($k \to h_{2v}$) of u_+ is sufficient; it is

$$u_+ \sim \frac{B_v}{\mathrm{i}\mu C_{2v}(r_{2v-1} - h_{2v})}\sqrt{0 - \mathrm{i}(k - h_{2v})}, \tag{136}$$

$$C_{2v} = \lim_{k\to h_{2v}} L_+(k)\sqrt{0 - \mathrm{i}(k - h_{2v})}$$

and the corresponding dissipative wave for $n \geq 0$, $\eta \to \infty$ is defined by

$$u_n(\eta) \sim \frac{1}{2\pi}\int_{-\varepsilon}^{\varepsilon} u_+(k)\exp(-nh(k) - \mathrm{i}k\eta)\,\mathrm{d}k. \tag{137}$$

Comparing this with (130) and (129) one can find that

$$u_n(\eta) \sim \frac{B_v \exp(-\mathrm{i}h_{2v}\eta)}{\mathrm{i}\sqrt{\pi}\mu C_{2v}(r_{2v-1} - h_{2v})}\frac{\mathrm{d}}{\mathrm{d}\eta}\frac{\exp(-\mathrm{i}\beta_0^2/4)}{\sqrt{\eta}}$$

$$= \frac{B_v \exp(-\mathrm{i}h_{2v}\eta)}{\sqrt{\pi}\mu C_{2v}(r_{2v-1} - h_{2v})}\frac{1}{\sqrt{\eta}}\left[\frac{(h^0)^2 n^2}{\eta^2} + \frac{\mathrm{i}}{2\eta}\right]\exp(-\mathrm{i}\beta_0^2/4). \tag{138}$$

It can be seen that the amplitude of this dissipative wave decreases as $\eta^{-3/2}$ at $n = 0$. However, for a non-zero n/η (even it is small as assumed) the amplitude decreases much slower, namely, as $\eta^{-1/2}$. This evidences that the wave carries energy to the 'north-east', i.e. ahead the crack front and away from the crack continuation.

The description of other dissipative waves as outlined in (106) by their trace at $n = 0$ can be obtained by similar considerations as above, and we do not dwell on that.

3.10. Conclusion. Existence of the solutions

In the above considerations, complex expressions for the feeding and dissipative waves were obtained. Taking into account the fact that the set of the singular points

of the function $L(k)$ consists of pairs ($k=\pm k_0$), one can come to real expressions. Consider a term in (72) corresponding to a feeding wave, say

$$p_+=\frac{2B_v}{L_+(k)[0-\mathrm{i}(k-r_{2v-1})]},\quad u_-=\frac{B_vL_-(k)}{\mu[0+\mathrm{i}(k-r_{2v-1})]}. \tag{139}$$

If this solution exists, the same solution with pole $k=-r_{2v-1}$ exists as well. We can put for the first solution (139)

$$B_v=\frac{L_+(r_{2v-1})p_v}{4}\mathrm{e}^{-\mathrm{i}\phi}, \tag{140}$$

where p_v and ϕ are real constants, and a conjugate complex value for second one [see equalities (49) which are also valid for $L_\pm$]. As a result we obtain

$$p_+(k)=\frac{pvL_+(r_{2v-1})}{2L_+(k)[0-\mathrm{i}(k-r_{2v-1})]}\mathrm{e}^{-\mathrm{i}\phi}+\frac{pvL_+(-r_{2v-1})}{2L_+(k)[0-\mathrm{i}(k+r_{2v-1})]}\mathrm{e}^{\mathrm{i}\phi},$$

$$u_-(k)=\frac{p_vL_+(r_{2v-1})L_-(k)}{4\mu[0+\mathrm{i}(k-r_{2v-1})]}\mathrm{e}^{-\mathrm{i}\phi}+\frac{p_vL_+(-r_{2v-1})L_-(k)}{4\mu[0+\mathrm{i}(k+r_{2v-1})]}\mathrm{e}^{\mathrm{i}\phi}. \tag{141}$$

The feeding wave is now

$$p_{\mathrm{f}}(\eta)=p_vH(\eta)\cos(r_{2v-1}\eta+\phi). \tag{142}$$

In the determination of the dissipative waves of the same wavenumber, r_{2v-1}, (u_-) and of any other wavenumber, note that, as follows from (141) and (49)

$$p_+(-k)=\overline{p_+(k)},\quad u_-(-k)=\overline{u_-(k)}. \tag{143}$$

This leads to the conclusion that the sum of contributions of singular points $k=k_0$ and $k=-k_0$ represents a real dissipative wave. This is valid not only for the line $n=0$ but for the x,y-plane as well since λ (29) satisfies the same relation as in (143).

We now have the following results:

$$p(+0)=\lim_{s\to\infty}sp_+(\mathrm{i}s)=p_v\Re\,(L_+(r_{2v-1})\mathrm{e}^{-\mathrm{i}\phi}),$$

$$p(\eta)\sim p_v\cos(r_{2v-1}\eta+\phi)\quad(\eta\to\infty). \tag{144}$$

A necessary condition for the existence of the solution is thus

$$\Re L_+(r_{2v-1})>1. \tag{145}$$

In this case, the internal force at the crack tip can exceed that for $\eta\to\infty$, at least, for $\phi=0$. Let the feeding wave amplitude, p_v, be given as well as the limiting force, p_{c}. It is clear that the crack cannot grow if

$$p_v\Re L_+(r_{2v-1})<p_{\mathrm{c}}. \tag{146}$$

In the opposite case

$$p_v\Re L_+(r_{2v-1})>p_{\mathrm{c}}, \tag{147}$$

phase ϕ is defined by the condition

$$\Re\,(L_+(r_{2v-1})\mathrm{e}^{-\mathrm{i}\phi})=\frac{p_{\mathrm{c}}}{p_v}>1. \tag{148}$$

Note that the above conditions for existence of the steady-state solution are necessary but not sufficient. For the determination of the sufficient conditions, a study of the function $p(\eta)$ is required, whether it reaches maximum at $\eta = 0$ or earlier. Besides, one has to observe whether the force in other bonds is sub-critical or not. In particular, this concerns the lines $n = 0$ and $n = -1$. It should be emphasized, however, that this requirement is based on the assumption that the strength of a bond is defined by a limiting force.

Acknowledgements

This research (No. 28/00-1) was supported by The Israel Science Foundation.

Appendix A. Causality principle for steady-state solutions

A steady-state solution is not unique if a homogeneous solution as a free wave exists. The existence of such waves, which can propagate, say, in the x-direction, reflects itself by singular points on the real k-axis of the Fourier transform. In the following, we consider both cases where x is a continuous or discrete coordinate; in the latter case, $x = an,\ n = 0, \pm 1, \ldots$.

For a steady-state solution of the type $u = u_0(\eta)\exp(\mathrm{i}\omega t)$, where ω is the frequency in the moving coordinate system, η, t, and $\eta = x - vt$, the uniqueness can be achieved in various ways, in particular, by the use of a rule based on the causality principle. Under this principle the solution is considered as a limit ($t \to \infty$, $\eta = \mathrm{const}$) of the solution to the corresponding transient problem with zero initial conditions.

Represent the steady-state solution as

$$u = u_0 \mathrm{e}^{\mathrm{i}\omega t}, \quad u_0(\eta) = g(\eta) * P(\eta), \tag{A.1}$$

where $P(\eta)\mathrm{e}^{\mathrm{i}\omega t}$ is an external force and the symbol $*$ denotes the convolution with respect to η.

Similarly, the transient solution can be represented as

$$U(t,x) = U_0(t,x)\mathrm{e}^{\mathrm{i}\omega t} = f(t,x) * *[P(x - vt)\mathrm{e}^{\mathrm{i}\omega t}], \tag{A.2}$$

where the symbol $**$ denotes the double convolution with respect to coordinate x and time t.

Suppose that the latter solution, considered in the moving coordinate system, has a limit, namely, for any finite η

$$\lim_{t\to\infty} U_0(t, \eta + vt) = u_0(\eta). \tag{A.3}$$

Each of these functions is assumed to be 'slowly growing': it grows (if it grows) slower than any exponential function.

For the *continuous case* consider the Fourier transform in the moving coordinate system

$$u_0^{\mathrm{F}*}(k) = \int_{-\infty}^{\infty} u_0(\eta)\mathrm{e}^{\mathrm{i}k\eta}\,\mathrm{d}\eta = g^{\mathrm{F}*}(k)P^{\mathrm{F}*}(k) \tag{A.4}$$

and the double-Laplace (with parameter s) and Fourier (with parameter k)-transformation of the transient solution

$$U^{\mathrm{LF}}(s,k)=\int_0^\infty\int_{-\infty}^\infty U(t,x)\mathrm{e}^{\mathrm{i}kx-st}\,\mathrm{d}x\,\mathrm{d}t=f^{\mathrm{LF}}(s,k)\frac{P^{\mathrm{F}*}(k)}{s-\mathrm{i}\Omega},\tag{A.5}$$

where $\Omega=kv+\omega$ is the frequency from an unmoving observer's point of view.

The inverse formula is

$$U(t,x)=\frac{1}{4\pi^2\mathrm{i}}\int_{-\infty}^\infty\int_{-\mathrm{i}\infty+0}^{\mathrm{i}\infty+0}f^{\mathrm{LF}}(s,k)\frac{P^{\mathrm{F}*}(k)}{s-\mathrm{i}\Omega}\mathrm{e}^{st-\mathrm{i}kx}\,\mathrm{d}s\,\mathrm{d}k.\tag{A.6}$$

The substitutions $s=s'+\mathrm{i}\Omega$ and $x=\eta+vt$ lead to the equality

$$U_0(t,\eta+vt)=\frac{1}{4\pi^2\mathrm{i}}\int_{-\infty}^\infty\int_{-\mathrm{i}\infty+0}^{\mathrm{i}\infty+0}\frac{P^{\mathrm{F}*}(k)}{s'}f^{\mathrm{LF}}(s'+\mathrm{i}\Omega,k)\mathrm{e}^{s't-\mathrm{i}k\eta}\,\mathrm{d}s'\,\mathrm{d}k.\tag{A.7}$$

and hence

$$U_0^{\mathrm{LF}*}(s,k)=\int_{-\infty}^\infty\int_0^\infty U(t,\eta+vt)\mathrm{e}^{-st+\mathrm{i}k\eta}\,\mathrm{d}t\,\mathrm{d}\eta=\frac{P^{\mathrm{F}*}(k)}{s}f^{\mathrm{LF}}(s+\mathrm{i}\Omega,k).\tag{A.8}$$

Further, we use the following theorem known in the Laplace transform theory:

If the limit $(t\to\infty)$ *of the function* w *exists then the limit of* $sw^{\mathrm{L}}(s)$ *also exists and*

$$\lim_{t\to\infty}w=\lim_{s\to+0}sw^{\mathrm{L}}(s).\tag{A.9}$$

In our case, as follows from (A.3), (A.4) and (A.8), the theorem leads to the final relation

$$g^{\mathrm{F}*}(k)=\lim_{s\to+0}f_0^{\mathrm{LF}*}(s,k)=f^{\mathrm{LF}}(0+\mathrm{i}\Omega,k),\quad\Omega=kv+\omega.\tag{A.10}$$

The causality principle runs thus: *the expression* $\mathrm{i}\Omega\equiv\mathrm{i}kv+\mathrm{i}\omega$ *in the* F_**-transform of the steady-state solution must be supplemented by* $+0$. In other words, *the frequency must be considered as having a vanishing negative imaginary part, that is,* – *as* $\Omega-\mathrm{i}0$.

Consider, for example, the one-dimensional wave equation with the moving and oscillating external force

$$\frac{\partial^2U}{\partial t^2}-\frac{\partial^2U}{\partial x^2}=P(x-vt)\mathrm{e}^{\mathrm{i}\omega t}.\tag{A.11}$$

The steady-state solution $u=u_0(\eta)\mathrm{e}^{\mathrm{i}\omega t}$ is defined by the following Fourier transform:

$$u_0^{\mathrm{F}*}(k)=P^{\mathrm{F}*}(k)g^{\mathrm{F}*}(k),\quad g^{\mathrm{F}*}(k)=\frac{1}{k^2+(\mathrm{i}kv+\mathrm{i}\omega)^2}\tag{A.12}$$

with singular points $k=\omega/(1-v)$ and $k=-\omega/(1+v)$ on the real k-axis. At the same time, under the rule (A.10) the function $g^{\mathrm{F}*}$ must be represented as

$$g^{\mathrm{F}*}(k)=\frac{1}{k^2+(0+\mathrm{i}kv+\mathrm{i}\omega)^2}\tag{A.13}$$

with singular points $k=\omega/(1-v)-\mathrm{i}0$ and $k=-\omega/(1+v)+\mathrm{i}0$. These expressions for the singular points represent a correct definition of the Fourier transform which can be used in the inverse transformation.

For the *discrete case*, $x = an$, we define $\eta = (x - vt)/a = n - vt/a$ and represent the transient solution in the form

$$U = U_0(t,n)\mathrm{e}^{\mathrm{i}\omega t} = f(t,n) * *[P(n - vt/a)\mathrm{e}^{\mathrm{i}\omega t}], \tag{A.14}$$

where the symbol $**$ denotes the double convolution with respect to n and t. The integral transform is

$$U^{\mathrm{LF_d}}(s,k) = \int_0^\infty \sum_{n=-\infty}^{\infty} U(t,n)\mathrm{e}^{\mathrm{i}kn - st}\,\mathrm{d}t. \tag{A.15}$$

Here and below the superscripts F_d and $F_{\mathrm{d}*}$ denote the discrete Fourier transform in the stationary and moving coordinate systems, respectively.

Let us represent the inverse formula as

$$\begin{aligned} U(t,n) &= \frac{1}{4\pi^2\mathrm{i}} \int_{-\pi}^{\pi} \int_{-\mathrm{i}\infty+0}^{\mathrm{i}\infty+0} U^{\mathrm{LF_d}}(s,k)\mathrm{e}^{st-\mathrm{i}kn}\,\mathrm{d}s\,\mathrm{d}k \\ &= \frac{1}{4\pi^2\mathrm{i}} \sum_{m=-\infty}^{\infty} \int_{-\pi}^{\pi} \left[\int_{s_m-\mathrm{i}\pi+0}^{s_m+\mathrm{i}\pi+0} U^{\mathrm{LF_d}}(s,k)\mathrm{e}^{st-\mathrm{i}kn}\,\mathrm{d}s \right] \mathrm{d}k \end{aligned} \tag{A.16}$$

with $s_m = \mathrm{i}(kv/a + \omega + 2\pi m)$. Substitute

$$k = l - 2\pi m, \quad s = s' + \mathrm{i}lv/a + \mathrm{i}\omega + 2\pi\mathrm{i}m. \tag{A.17}$$

For any integer m and n

$$\mathrm{e}^{2\pi\mathrm{i}m} = 1, \quad U^{\mathrm{LF_d}}(s + 2\pi\mathrm{i}m, k + 2\pi n) = U^{\mathrm{LF_d}}(s,k) \tag{A.18}$$

and hence

$$\begin{aligned} U_0(t,n) &= \frac{1}{4\pi^2\mathrm{i}} \sum_{m=-\infty}^{\infty} \int_{(2m-1)\pi}^{(2m+1)\pi} \left[\int_{-\mathrm{i}\pi+0}^{\mathrm{i}\pi+0} U^{\mathrm{LF_d}}(s' + \mathrm{i}lv/a + \mathrm{i}\omega, l)\mathrm{e}^{s't}\,\mathrm{d}s' \right] \mathrm{e}^{-\mathrm{i}l\eta}\,\mathrm{d}l \\ &= \frac{1}{4\pi^2\mathrm{i}} \int_{-\mathrm{i}\pi+0}^{\mathrm{i}\pi+0} \left[\int_{-\infty}^{\infty} U^{\mathrm{LF_d}}(s' + \mathrm{i}lv/a + \mathrm{i}\omega, l)\mathrm{e}^{-\mathrm{i}l\eta}\,\mathrm{d}l \right] \mathrm{e}^{s't}\,\mathrm{d}s'. \end{aligned} \tag{A.19}$$

This expression is the inverse formula for the double transform: the continuous Fourier transform with respect to η and the discrete Laplace transform with respect to t. Theorem (A.9) is valid for the discrete case; hence the rule (A.10) is valid for the discrete case as well.

Appendix B. Pre-limiting location of a zero point and the group velocity

Consider an analytic function $f(\mathrm{i}\Omega, k)$ ($\Omega = kV$, $\omega = 0$) with dispersion relation $\Omega = \Omega(k)$ defined by the equality

$$f(\mathrm{i}\Omega, k) = 0. \tag{B.1}$$

Note that the group velocity is given by $V_g = d\Omega/dk$, while the phase velocity by $V = \Omega/k$. Successive differentiation of equality (168) leads to a sequence of relations:

$$\frac{\partial f}{\partial \Omega} V_g + \frac{\partial f}{\partial k} = 0,$$

$$\frac{\partial^2 f}{\partial \Omega^2} V_g^2 + \frac{\partial f}{\partial \Omega} \frac{dV_g}{dk} + 2\frac{\partial^2 f}{\partial \Omega \partial k} V_g + \frac{\partial^2 f}{\partial k^2} = 0,$$

$$\dots \tag{B.2}$$

Consider a point, $k_0,\ \Omega_0 = \Omega(k_0)$, on the dispersion curve where these values are real. Following the rule based on the causality principle (A.10), we find a pre-limiting expression for the function f as $f(p + i\Omega, k),\ p \to +0$. Let the root of the equation

$$f(p + i\Omega, k) = 0 \tag{B.3}$$

be $k = k_0 + \delta k(p)$ $(\delta k(0) = 0)$. We can represent

$$\begin{aligned} f(p + i\Omega, k) &= f(p + i\Omega_0 + i\delta k V,\ k_0 + \delta k) \\ &= \frac{\partial f}{\partial \Omega}(\delta k V - ip) + \frac{\partial f}{\partial k}\delta k + \frac{1}{2}\left[\frac{\partial^2 f}{\partial \Omega^2}(\delta k V - ip)^2 + \frac{\partial^2 f}{\partial k^2}\delta k^2 \right. \\ &\quad \left. + 2\frac{\partial^2 f}{\partial \Omega \partial k}\delta k(\delta k V - ip)\right] + \dots = 0. \end{aligned} \tag{B.4}$$

Note that in this variation $V =$ const and the derivatives are considered at the point $k = k_0,\ \Omega = \Omega_0$.

Consider some particular cases related to the problem of crack propagation in the lattice. Let the following inequalities be valid:

$$\partial f/\partial \Omega \neq 0, \quad V \neq V_g. \tag{B.5}$$

In this case, only the terms with derivatives of the first order are to be taken into account; using the first equality in (B.2) we get

$$\delta k \sim \frac{ip}{V - V_g} \quad (p \to +0). \tag{B.6}$$

Thus under conditions (B.5) the zero point $k = k_0$ comes to the real axis from below if $V < V_g$ and vice versa.

Let the second case be

$$\partial f/\partial \Omega \neq 0, \quad V = V_g, \quad dV_g/dk \neq 0. \tag{B.7}$$

From (B.2) and (B.4) it follows that

$$\delta k \sim \pm\sqrt{\frac{2iVp}{dV_g/dk}} \quad (p \to +0). \tag{B.8}$$

It can be seen that $k = k_0$ is now a limiting location of two roots. One of them comes from above and the other from below.

Equalities (B.6) and (B.8) allow one to determine the pre-limiting position of a zero point directly from the behaviour of dispersion curves as shown in Fig. 5. Note that the condition $\partial f/\partial\Omega \neq 0$ is usually satisfied for $\Omega \neq 0$.

Next, consider

$$\frac{\partial f}{\partial \Omega} = \frac{\partial^2 f}{\partial \Omega\, \partial k} = 0, \quad \frac{\partial^2 f}{\partial \Omega^2} \neq 0, \quad V \neq V_{\mathrm{g}}. \tag{B.9}$$

Here, there is a double root as above:

$$\delta k = \delta k_{1,2}, \quad \delta k_1 \sim \frac{\mathrm{i}p}{V - V_{\mathrm{g}}}, \quad \delta k_2 \sim \frac{\mathrm{i}p}{V + V_{\mathrm{g}}} \ (p \to +0). \tag{B.10}$$

In contrast to the previous case, the roots belong to different half-planes only if $V < V_{\mathrm{g}}$.

Finally, consider a four-fold root of the function $h^2 = 2(1 - \cos k) + (s + \mathrm{i}kV)^2 (V = v/c, s \to +0)$ (26) in the case $V = 1$. From (B.2) and (B.4) or directly from the expression for h^2 (26) it follows that

$$\frac{1}{12}\delta k^4 - 2\mathrm{i}p\delta k - p^2 = 0,$$

$$\delta k_m \sim (24p)^{1/3} \exp[\tfrac{1}{3}\mathrm{i}\pi(\tfrac{1}{2} + 2(m-1))], \ \ m = 1,2,3; \ \ \delta k_4 \sim \frac{\mathrm{i}p}{2} \ (p \to +0). \tag{B.11}$$

Thus, in this case one of the roots belongs to the lower half-plane and three other roots belong to the upper one.

It can be seen that in the single-root case (B.5), the rule (A.10) coincides with the Mandelshtam principle (Mandelshtam, 1972) which requires that *waves must carry energy to infinity*. Indeed, for an inhomogeneous equation

$$f(\mathrm{i}\Omega, k) u^{\mathrm{F}*}(k) = P^{\mathrm{F}*}(k), \tag{B.12}$$

the Fourier transform of the wave, u, associated with this wavenumber, $k = k_0$, has a singular point in the lower (upper) half-plane if $V < V_{\mathrm{g}}$ ($V > V_{\mathrm{g}}$) [see (B.6)]. Consequently, the wave is located at $\eta > 0$ ($\eta < 0$) and carries energy with the group to the right (to the left), that is, to infinity but not from infinity. In a general case, direct use of the Mandelshtam principle for the determination of the pre-limiting locations of singular and zero points on the real k-axis is difficult.

Appendix C. Arising of the delta-function

Consider functions

$$f_+(s,k) = \frac{(2s)^v}{[s - \mathrm{i}(k - k_0)]^{v+1}}, \quad f_-(s,k) = \frac{(2s)^v}{[s + \mathrm{i}(k - k_0)]^{v+1}},$$

$$f_\pm(s,k) = \frac{(2s)^v}{[s - \mathrm{i}(k - k_0)][s + \mathrm{i}(k - k_0)]^v},$$

$$f_\mp(s,k) = \frac{(2s)^v}{[s + \mathrm{i}(k - k_0)][s - \mathrm{i}(k - k_0)]^v}, \tag{C.1}$$

where k_0 is a real constant, $v>0$. In the limit, $s=+0$, these functions as distributions become

$$f_+(+0,k)=f_-(+0,k)=0,$$

$$f_\pm(+0,k)=f_\mp(+0,k)=2\pi\delta(k-k_0)=\frac{1}{0+\mathrm{i}(k-k_0)}+\frac{1}{0-\mathrm{i}(k-k_0)}. \quad (C.2)$$

Indeed, when $s\to+0$ each of these functions tends to zero everywhere except at the point $k=k_0$ where it tends to infinity. At the same time, these functions are locally integrable independently of s and

$$\int_\infty^\infty f_+(s,k)\,\mathrm{d}k=\int_\infty^\infty f_-(s,k)\,\mathrm{d}k=\int_\infty^\infty\frac{2^v}{(1-\mathrm{i}x)^{v+1}}=0,$$

$$\int_\infty^\infty f_\pm(s,k)\,\mathrm{d}k=\int_\infty^\infty f_\mp(s,k)\,\mathrm{d}k=\int_\infty^\infty\frac{2^v}{(1-\mathrm{i}x)(1+\mathrm{i}x)^v}=2\pi. \quad (C.3)$$

Appendix D. Functions S and λ at zero points of $h(k)$ and $r(k)$

The function $S(k)$ defined by (57) is

$$S(k)=\frac{H_+(k)H_-(k)r(k)}{R_+(k)R_-(k)h(k)}. \quad (D.1)$$

Both the numerator and denominator of this fraction are equal to zero if $h(k)=0$ ($r=2$) or $r(k)=0$ ($h=2\mathrm{i}\,\mathrm{sign}\,k$). To find the ratio, consider asymptotes of these functions in a vicinity of a zero point for the case of a nonzero simple root. For $k\to h_{2v-1}$

$$h^2(k)\sim\mathrm{d}[h^2(h_{2v-1})]/\mathrm{d}k(l-\mathrm{i}0)=2(\sin h_{2v-1}-h_{2v-1}V^2)(l-\mathrm{i}0)$$

$$=2h_{2v-1}V(V_\mathrm{g}-V)(l-\mathrm{i}0),$$

$$S(h_{2v-1})=2[-R_+^2(h_{2v-1})R_-^2(h_{2v-1})h_{2v-1}^2V(V-V_\mathrm{g})]^{-1/2}C_1,$$

$$C_1=\sqrt{H_+^2(h_{2v-1})\prod_{\mu\neq v}^{l+1}\left[1-\left(\frac{h_{2\mu-1}}{h_{2v-1}}\right)^2\right]}, \quad (D.2)$$

where $l=k-h_{2v-1}$ and V_g is the group velocity. Note that here and below each expression under the square root is positive. Similarly, for $k\to h_{2v}$ where $V_\mathrm{g}>V$

$$h^2(k)\sim\mathrm{d}[h^2(h_{2v})]/\mathrm{d}k(l+\mathrm{i}0)=2h_{2v}V(V_\mathrm{g}-V)(l+\mathrm{i}0),$$

$$S(h_{2v})=2[-R_+^2(h_{2v})R_-^2(h_{2v})h_{2v}^2V(V_\mathrm{g}-V)]^{-1/2}C_2,$$

$$C_2=\sqrt{-H_-^2(h_{2v})\prod_{\mu\neq v}^{l}\left[1-\left(\frac{h_{2\mu}}{h_{2v}}\right)^2\right]}, \quad (D.3)$$

where $l = k - h_{2v}$. In addition, in a vicinity of a real root of the equation $h(k) = 0$,

$$\lambda = \frac{r-h}{r+h} \sim \frac{1-h/2}{1+h/2} \sim \mathrm{e}^{-h}. \tag{D.4}$$

In a vicinity of $k = r_{2v-1}$ or $k = r_{2v}$ where $h^2 \sim -4$

$$r^2(k) \sim \mathrm{d}[r^2(r_{2v-1})]/\mathrm{d}k(l - \mathrm{i}0) = 2(\sin r_{2v-1} - r_{2v-1}V^2)(l - \mathrm{i}0)$$
$$= 2r_{2v-1}V(V_\mathrm{g} - V)(l - \mathrm{i}0),$$

$$S(r_{2v-1}) = \frac{1}{2}H_+(r_{2v-1})H_-(r_{2v-1})\sqrt{r_{2v-1}^2 V(V - V_\mathrm{g})}C_3,$$

$$C_3 = \left(R_+^2(r_{2v-1})\prod_{\mu\neq v}^{d+1}\left[1 - \left(\frac{r_{2\mu-1}}{r_{2v-1}}\right)^2\right]\right)^{-1/2}, \tag{D.5}$$

where $l = k - r_{2v-1}$, and

$$r^2(k) \sim \mathrm{d}[r^2(r_{2v})]/\mathrm{d}k(l + \mathrm{i}0) = 2r_{2v}V(V_\mathrm{g} - V)(l + \mathrm{i}0),$$
$$S(r_{2v}) = \frac{1}{2}H_+(r_{2v})H_-(r_{2v})\sqrt{r_{2v}^2 V(V_\mathrm{g} - V)}C_4$$
$$C_4 = \left(-R_-^2(r_{2v})\prod_{\mu\neq v}^{d+1}\left[1 - \left(\frac{r_{2\mu}}{r_{2v}}\right)^2\right]\right)^{-1/2}, \tag{D.6}$$

where $l = k - r_{2v}$. In these cases, in a vicinity of a real root of the equation $r(k) = 0$,

$$\lambda = \frac{r-h}{r+h} \sim -\frac{1+\mathrm{i}r/2}{1-\mathrm{i}r/2} \sim -\mathrm{e}^{\mathrm{i}r}. \tag{D.7}$$

References

Abraham, F.F., Gao, H., 2000. How fast can cracks propagate? Phys. Rev. Lett. 84, 3113–3116.

Broberg, K.B., 1999. Cracks and Fracture. Academic Press, San Diego.

Freund, L.B., 1990. Dynamic Fracture Mechanics. Cambridge University Press, Cambridge.

Kessler, D.A., Levine, H., 2000. Nonlinear lattice model of viscoelastic Mode III fracture. http://xxx.tau.ac.il/ [Physics, cond-mat/0007149].

Kulakhmetova, S.A., Saraikin, V.A., Slepyan, L.I., 1984. Plane problem of a crack in a lattice. Mech. Solids 19, 101–108.

Mandelshtam, L.I., 1972. Lectures on Optics, Theory of Relativity and Quantum Mechanics. Nauka, Moscow (in Russian).

Marder, M., Gross, S., 1995. Origin of crack tip instabilities. J. Mech. Phys. Solids 43, 1–48.

Pechenik, L., Levine, H., Kessler, D.A., 2000a. Steady-state mode III cracks in a viscoelastic lattice model. Represented in the Internet: http://xxx.tau.ac.il/ [Physics, cond-mat/0002313].

Pechenik, L., Levine, H., Kessler, D.A., 2000b. Steady-state mode III cracks in a viscoelastic lattice model. Represented in the Internet: http://xxx.tau.ac.il/ [Physics, cond-mat/0002314].

Ravi-Chandar, K., Knauss, W.G., 1984. An experimental investigation into dynamic fracture: III. On steady-state crack propagation and crack branching. Int. J. Frac. 26, 141–154.

Slepyan, L.I., 1981a. Dynamics of a crack in a lattice. Soviet Phys. Dokl. 26, 538–540.

Slepyan, L.I., 1981b. Crack propagation in high-frequency lattice vibrations. Soviet Phys. Dokl. 26, 900–902.
Slepyan, L.I., 1984. Dynamics of brittle fracture in media with a structure. Mech. Solids 19, 114–122.
Slepyan, L.I., 1998. Some basic aspects of crack dynamics. In: Cherepanov, G. (Ed.), FRACTURE: A Topical Encyclopedia of Current Knowledge Dedicated to Alan Arnold Griffith. Krieger, Melbourne, USA, pp. 620–661.
Slepyan, L.I., 2000. Dynamic factor in impact, phase transition and fracture. J. Mech. Phys. Solids 48, 931–964.
Slepyan, L.I., Ayzenberg, M.V., Dempsey, J.P., 1999. A lattice model for viscoelastic fracture. Mech. Time-Dependent Materials 3, 159–203.
Slepyan, L.I., Troyankina, L.V., 1984. Fracture wave in a chain structure. J. Appl. Mech. Techn. Phys. 25, No. 6, 921–927.
Slepyan, L.I., Troyankina, L.V., 1988. Impact waves in a nonlinear chain. In: Goldstein, R.V. (Ed.), Strength and Visco-plasticity. Nauka, Moscow, pp. 301–305 (in Russian).